Medical Isotope Production at Berkeley

Andrew S. Voyles

19 May 2017

2017 Nuclear Physics Summer School in Oslo

Berkeley
UNIVERSITY OF CALIFORNIA

Overview

- Berkeley is currently leading a targeted experimental campaign to address these needs:
  - (n,p) production cross sections – UCB
  - Stacked-target charged particle excitation functions – LBNL / LANL
  - Tunable quasi-monoenergetic neutron source – LBNL

^{64}Cu and ^{47}Sc (n,p) Cross-Section Measurements for Medical Radionuclide Production

UCB

Some perspective

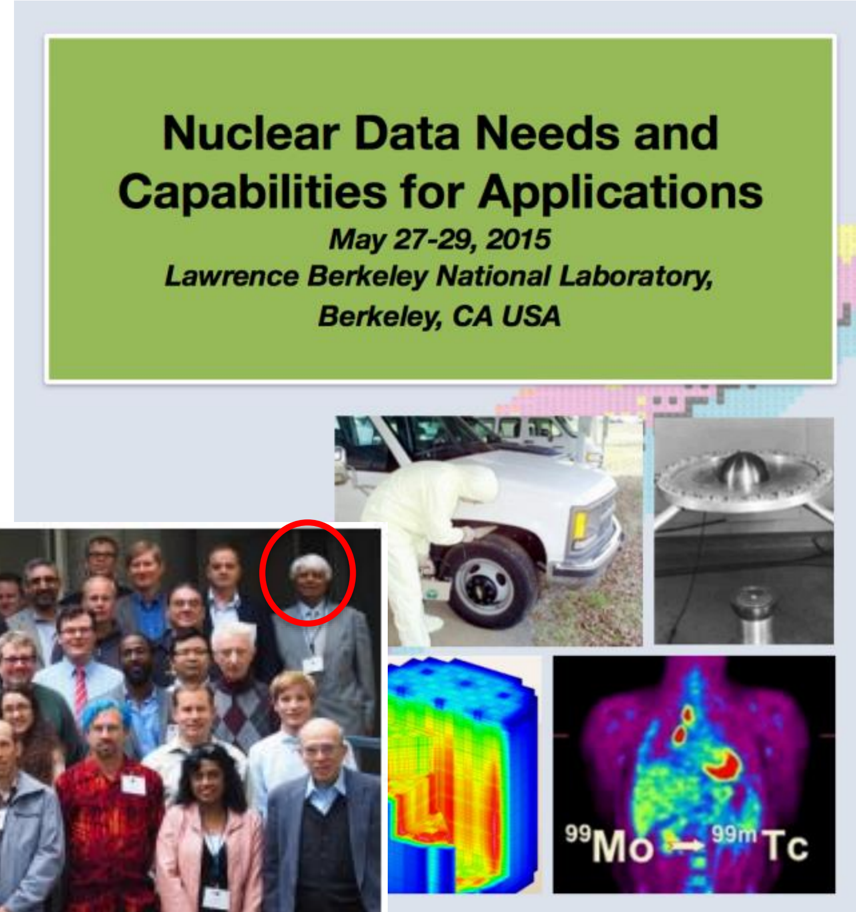

Some perspective

1. Charged-particle reactions for the production of medical isotopes at low energies (E < 30 MeV):
   - ^{45}Sc(p,n)^{45}Ti; ^{52}Cr(p,n)^{52}Mn; ^{54}Fe(d,n)^{55}Co; ^{67}Zn(p,α)^{64}Cu; ^{72}Ge(p,n)^{72}As, ^{74}Se(d,n)^{75}Br; ^{86}Sr(p,n)^{86}Y; ^{120}Te(p,n)^{120}I

^{32}S(n,p)^{32}P; ^{47}Ti(n,p)^{47}Ca, ^{64}Zn(n,p)^{64}Cu; ^{67}Zn(n,p)^{67}Cu; ^{89}Y(n,p)^{89}Sr, ^{105}Pd(n,p)^{105}Rh; ^{149}Sm(n,p)^{149}Pm, ^{153}Eu(n,p)^{153}Sm, ^{159}Tb(n,p)^{159}Gd; ^{161}Dy(n,p)^{161}Tb; ^{166}Er(n,p)^{166}Ho; ^{169}Tm(n,p)^{169}Er; ^{175}Lu(n,p)^{175}Yb; ^{177}Hf(n,p)^{177}Lu

4. Need small uncertainties on all dosimetry reactions

Highlight from WTTC 2016: ^{54}Fe(p,α)^{51}Mn

NDNCA Whitepaper available at http://bang.berkeley.edu/events/ndnca/whitepaper/

Isotope Production Needs

- ^{59}Co(p,3n)^{57}Ni, ^{75}As(p,3n)^{73}Se,
  ^{121}Sb(p,3n)^{119}Te/^{119}Sb, ^{133}Cs(p,3
- ^{55}Mn(p,4n)^{52}Fe, ^{71}Ga(p,4n)^{68}Ge,
- ^{133}Cs(p,5n)^{128}Ba
- ^{127}I(p,6n)^{122}Xe
- ^{nat}Br(p,x)^{72}Se, ^{nat}In(p,x)^{110}Sn, ^{122}T
- ^{nat}Sb(p,xn)^{119}Te/^{119}Sb, ^{nat}La(p,xn
- ^{68}Zn(p,αn)^{64}Cu
- ^{68}Zn(p,2p)^{67}Cu, ^{124}Xe(p,2p)^{123}I
- ^{124}Xe(p,pn)^{123}Xe
- (p,x) reaction on $^{94-98}$Mo for imp
- ^{107}Ag(p,αn)^{103}Pd
- ^{116}Cd(α,3n)^{117m}Sn; ^{192}Os(α,3n)^{193}

3. Nuclear data needed for radionuclides fission neutrons:
   - ^{36}S(n,x)^{32}Si
   - ^{nat}Cl(n,x)^{32}Si, ^{37}Cl(n,x)^{32}Si
   - ^{nat}Zn(n,x)^{67}Cu, ^{68}Zn(n,x)^{67}Cu, ^{70}Z
   - ^{226}Ra(n,2n)^{225}Ra
   - ^{232}Th(n,x)^{225}Ac, ^{232}Th(n,x)^{227}Ac
   - ^{32}S(n,p)^{32}P; ^{47}Ti(n,p)^{47}Ca, ^{64}Zn(n,
     ^{149}Sm(n,p)^{149}Pm, ^{153}Eu(n,p)^{153}Sm
     ^{169}Tm(n,p)^{169}Er; ^{175}Lu(n,p)^{175}Yb;
4. High-energy photon-induced reactions
   - ^{68}Zn(γ,p)^{67}Cu; ^{100}Mo(γ,n)^{99}Mo;
5. Nuclear da
   - ^{100}Mo(α,p2n)
   - ^{100}Mo(n,2n)
   - ^{100}Mo(p,pn) - data on long-lived

7. Nuclear data needed for Super Heavy Element (SHE) target
   - ^{248}Cm(n,γ) low energy resonances
   - ^{249}Bk(n,γ)

Gamma yield spectrum for incident neutron energies in the heat generation rates:
- *Te(n,γ) (production of ^{131}I)
- *Mo(n,γ)
- *Ru(n,γ)
- ^{103}Rh(n,γ)
- ^{154}Eu(n,γ)
- ^{155}Eu(n,γ)
- ^{141}Ce(n,γ)
- ^{140}Ce(n,γ)
- *Sn(n,γ)

Note: * indicates stable isotopes

Excitation function for incident neutron energies from therm
- ^{177}Lu(n,γ), ^{154}Eu(n,γ), ^{155}Eu(n,γ), ^{77}As(n,γ), ^{72}As(n,γ),

1. ^{117}Sn(n,n'), covering energy response 0.3 – 3.0 MeV
2. Data to support new evaluations
   - ^{23}Na(n,γ), discrepant in fast neutron region, > 100 ke
   - ^{23}Na(n,2n)
   - ^{27}Al(n,2n)
3. Address discrepancies:

4. Need small uncertainties on all dosimetry reactions

n standard benchmark neutron field
^{31}P(n,p), ^{10}B(n,X)α, ^{54}Fe(n,α), ^{23}Na(n,2n), ^{186}W(n,γ),
Sc(n,γ), and ^{64}Zn(n,p)
ary
n,f) and ^{238}U(n,2n)

6. IRMM Exploratory Study of Validation Data in ^{252}Cf Standard Neutron Benchmark Field
   - Issues with existing ^{197}Au(n,γ) due to room return
   - Issues with existing ^{90}Zr(n,2n) due to Th contamination
   - Issue with existing ^{96}Zr(n,2n) due to ^{94}Zr(n,γ) contribution

Tc and ^{nat}Mo(α, X)^{97}Ru

8. Validation data in 30 keV MAC
   ^{238}U(n,γ)
9. Test and improve decay chara

10. Gamma Emission Probabilities
    - ^{103m}Rh -- X-ray emissi

    - ^{56}Fe, ^{54}Fe (ASTM E693
12. Uncertainty in recoil spectrum
    - Recoil spectrum chara
    - ^{69}Ga, ^{71}Ga, ^{75}As
    - Fe isotopes
    - Validate/test use of ca

Inertial Confinement Fusion Data Needs

1. Accurate, temperature-dependent fusion reactivity for light ions is of primary importance to describe thermonuclear burn.
   - d(t,α)n, t(t, α)2n, d(d,t)p, d(d,^{3}He)n, d(^{3}He, α)p

   - Xe dopants to probe ablation front instabilities.
   - Br(d,2n)Kr to probe ablator/cold fuel and ablator/hot core mix.
   - Alpha particle induced reactions to probe hot core mix: ^{6}Li, ^{9}Be, ^{10}B (best one), ^{12}C, ^{14}N, ^{16}O, ^{19}F, ^{20}Ne, ^{23}Na, ^{24}Mg, ^{27}Al.
4. Gamma-ray diagnostics for performance and ablator/fuel instabilities.
   - Total yield from d-t fusion γ branching ratio at 17.6 MeV.
   - ^{12}C(n,n'γ) 4.4 MeV time-integrated emission provides hydrocarbon areal densities (remaining mass). Cross section at 14 MeV must be accurate.
   - Does ^{13}C(n,n'γ) have strong emission near 4 MeV? If not, then a useful mix diagnostic is possible.
5. Solid Radiochemistry Diagnostic (SRC) is currently an NIF diagnostic complementary to ^{12}C-γ GRH detection (CH ρr).
   - Ratio of ^{198}Au/^{196}Au from the activated hohlraum.
   - (n,γ)/(n,2n):low energy neutrons/14 MeV neutrons.

Berkeley
UNIVERSITY OF CALIFORNIA

Cross-Section Systematics

$$R = N_T \sigma\left(\bar{E}\right)\phi\left(\bar{E}\right)$$

$$\begin{aligned} N_\gamma &= N_D \epsilon_\gamma I_\gamma \\ &= \epsilon_\gamma I_\gamma \frac{N_T \sigma\left(\bar{E}\right)\phi\left(\bar{E}\right)}{\lambda}\left(1 - e^{-\lambda t_i}\right) e^{-\lambda t_d}\left(1 - e^{-\lambda t_c}\right) \end{aligned}$$

$$\sigma\left(\bar{E}\right) = \frac{N_\gamma \lambda}{N_T \epsilon_\gamma I_\gamma \phi\left(\bar{E}\right)\left(1 - e^{-\lambda t_i}\right) e^{-\lambda t_d}\left(1 - e^{-\lambda t_c}\right)}$$

Medical Applications

- Emerging medical radionuclides
  - ^{64}Cu ($t_{1/2}$ = 12.7 hr) – 61% β^+ to ^{64}Ni, 39% β^- to ^{64}Zn
  - ^{47}Sc ($t_{1/2}$ = 3.35 d) – β^- to ^{47}Ti, with 159-keV γ

Promising Prospects for ^{44}Sc-/^{47}Sc-Based Theragnostics: Application of ^{47}Sc for Radionuclide Tumor Therapy in Mice

Cristina Müller[1], Maruta Bunka[2,3], Stephanie Haller[1], Ulli Köster[4], Viola Groehn[5], Peter Bernhardt[6,7], Nicholas van der Meulen[2], Andreas Türler[2,3], and Roger Schibli[1,8]

[1]Center for Radiopharmaceutical Sciences ETH-PSI-USZ, Paul Scherrer Institute, Villigen-PSI, Switzerland; [2]Laboratory of Radiochemistry and Environmental Chemistry, Paul Scherrer Institute, Villigen-PSI, Switzerland; [3]Laboratory of Radiochemistry and Environmental Chemistry, Department of Chemistry and Biochemistry University of Bern, Bern, Switzerland; [4]Institut Laue-Langevin, Grenoble, France; [5]Merck and Cie, Schaffhausen, Switzerland; [6]Department of Radiation Physics, The Sahlgrenska Academy, University of Gothenburg, Gothenburg, Sweden; [7]Department of Medical Physics and Medical Bioengeneeri University Hospital, Gothenburg, Sweden; and [8]Department of Chemistry and Applied Biosciences, ETH Zuric

In Vivo Evaluation of Pretargeted ^{64}Cu for Tumor Imaging and Therapy

Michael R. Lewis, PhD[1]; Mu Wang, MD[1]; Donald B. Axworthy, BS[2]; Louis J. Theodore, PhD[2]; Robert W. Mallet, BS[2]; Alan R. Fritzberg, PhD[2]; Michael J. Welch, PhD[1]; and Carolyn J. Anderson, PhD[1]

[1]Mallinckrodt Institute of Radiology, Washington University School of Medicine, St. Louis, Missouri; and [2]NeoRx Corporation, Seattle, Washington

The UC Berkeley High Flux Neutron Generator

2.45 MeV neutrons, 10^8 n/s/cm^2
Extraction Plate: 5mm diameter

Commissioning:
25 July 2015

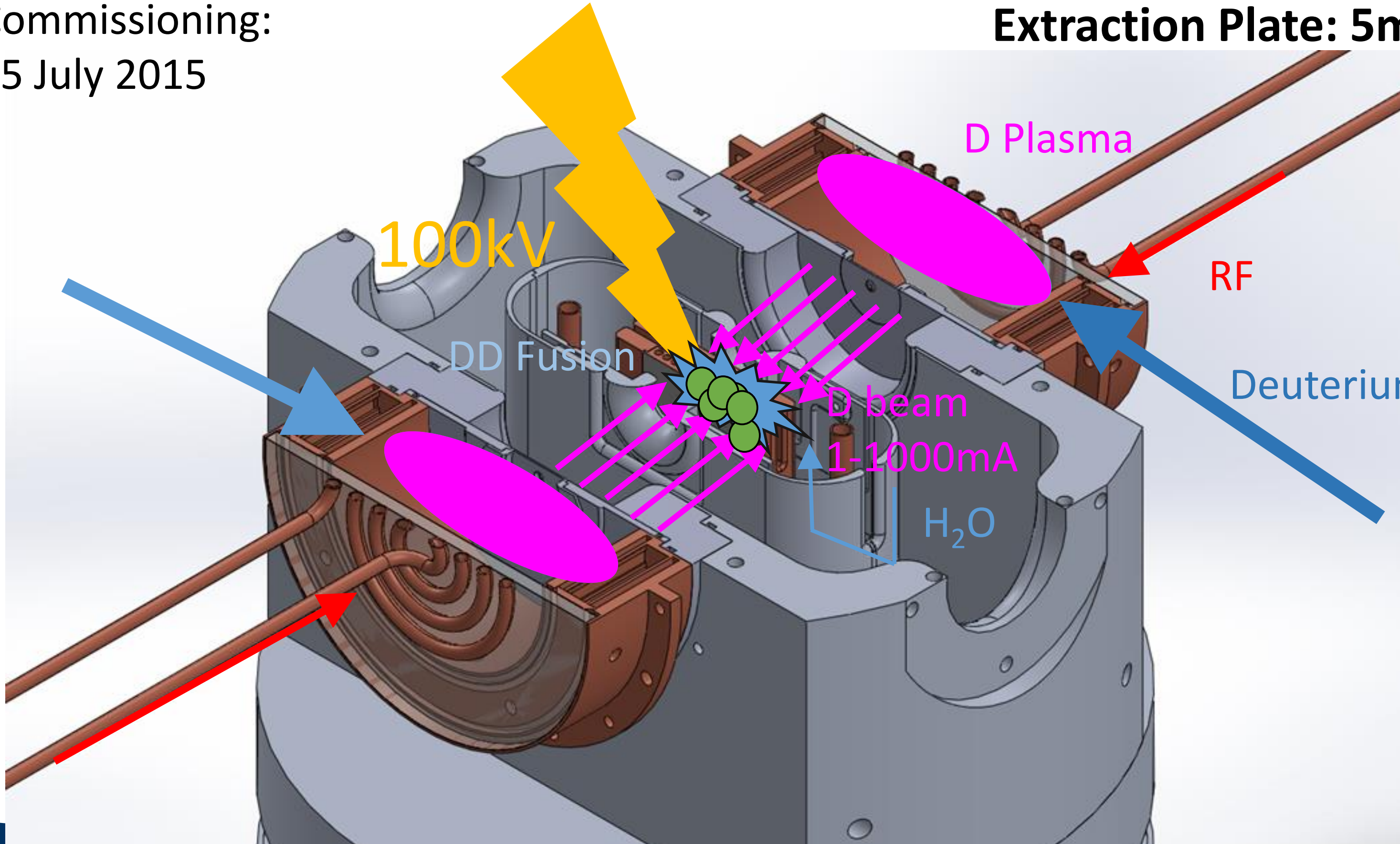

The UC Berkeley High Flux Neutron Generator

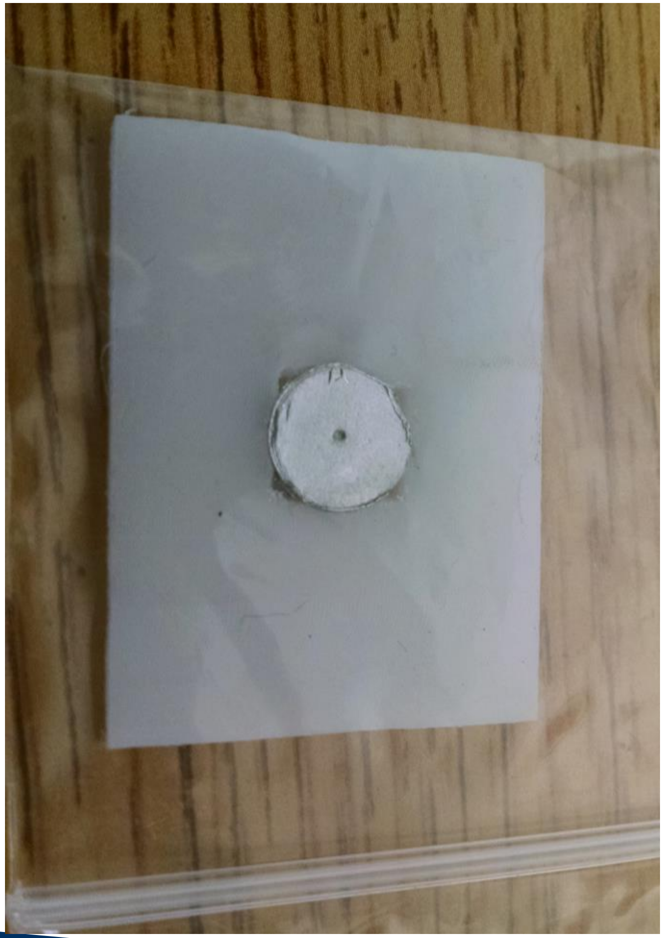

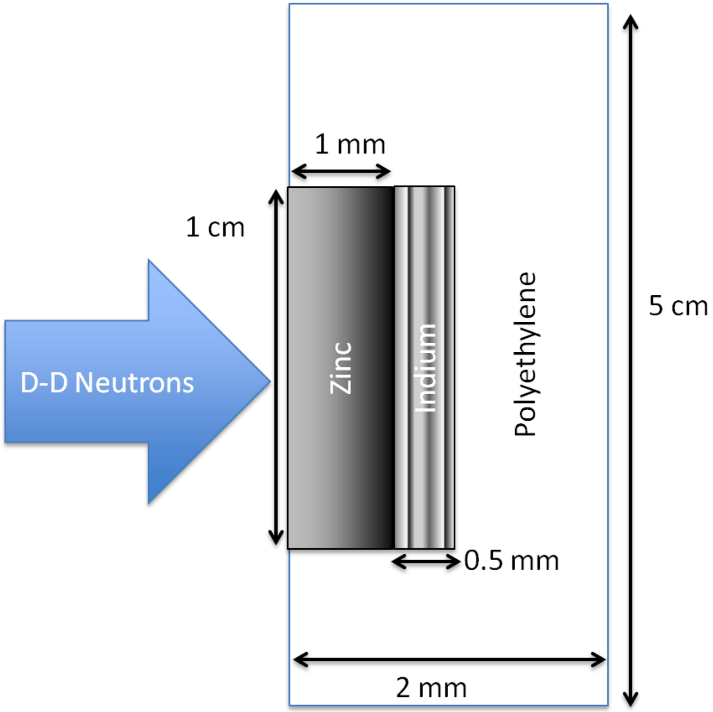

Foils Used	Metal Purity	Abundance (a/o)	Foil Density (mg/cm^2)
^{nat}In	> 99.999%	^{113}In (4.29%), ^{115}In (95.71%)	365.5
^{nat}Zn	> 99.99%	^{64}Zn (49.17%)	714.1
^{nat}Ti	99.999%	^{47}Ti (7.44%)	450.6

The UC Berkeley High Flux Neutron Generator

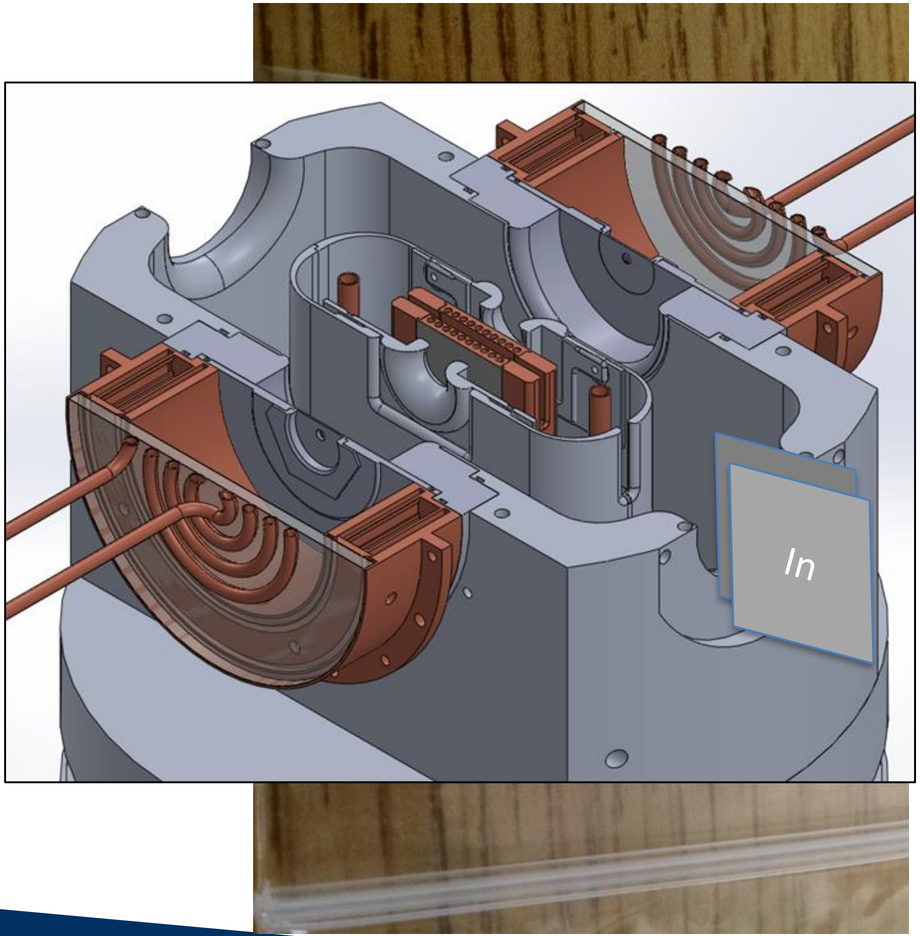

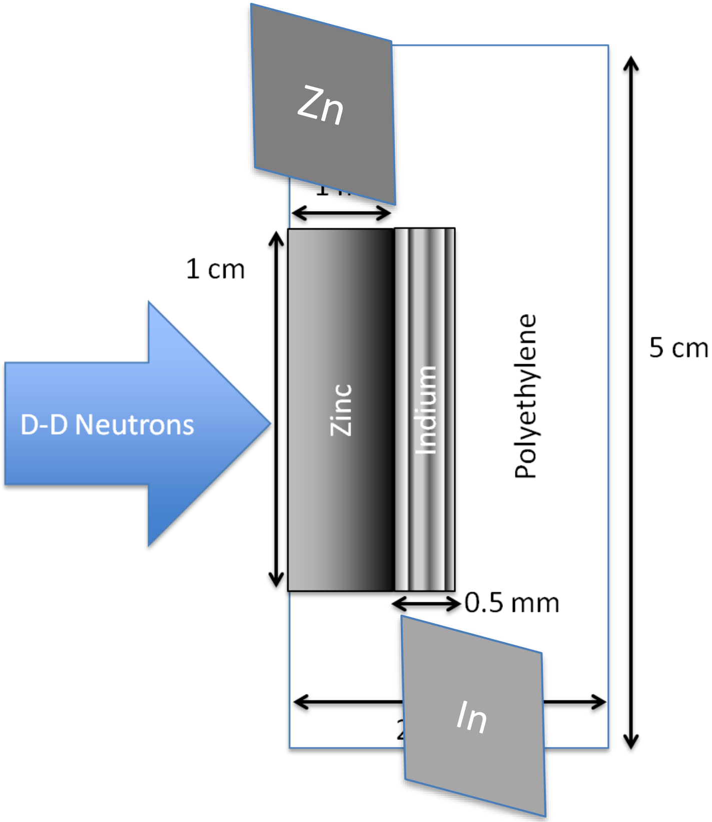

The UC Berkeley High Flux Neutron Generator

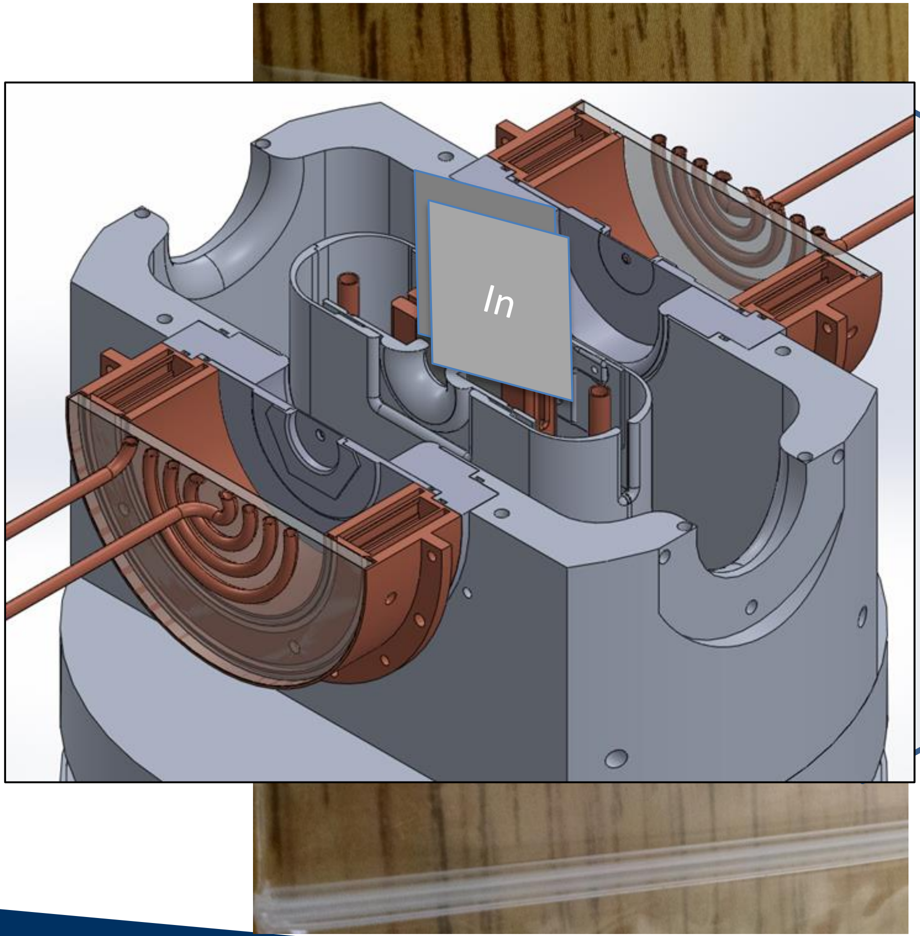

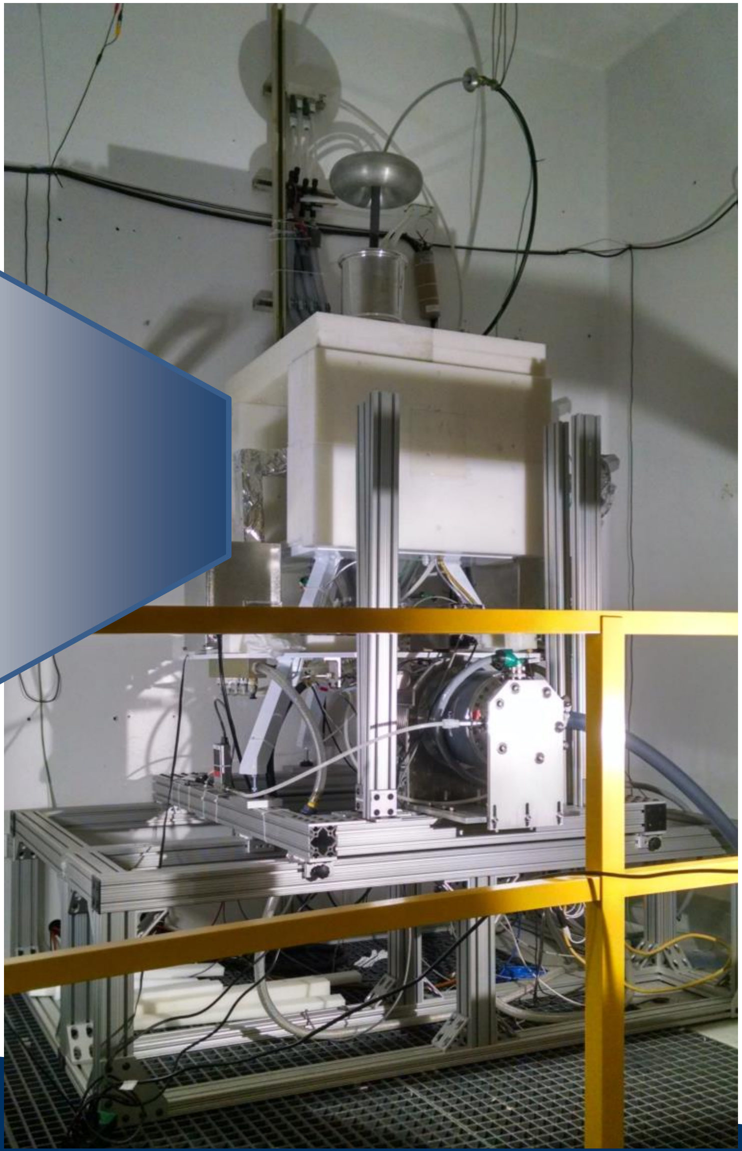

Relative Activation Measurements

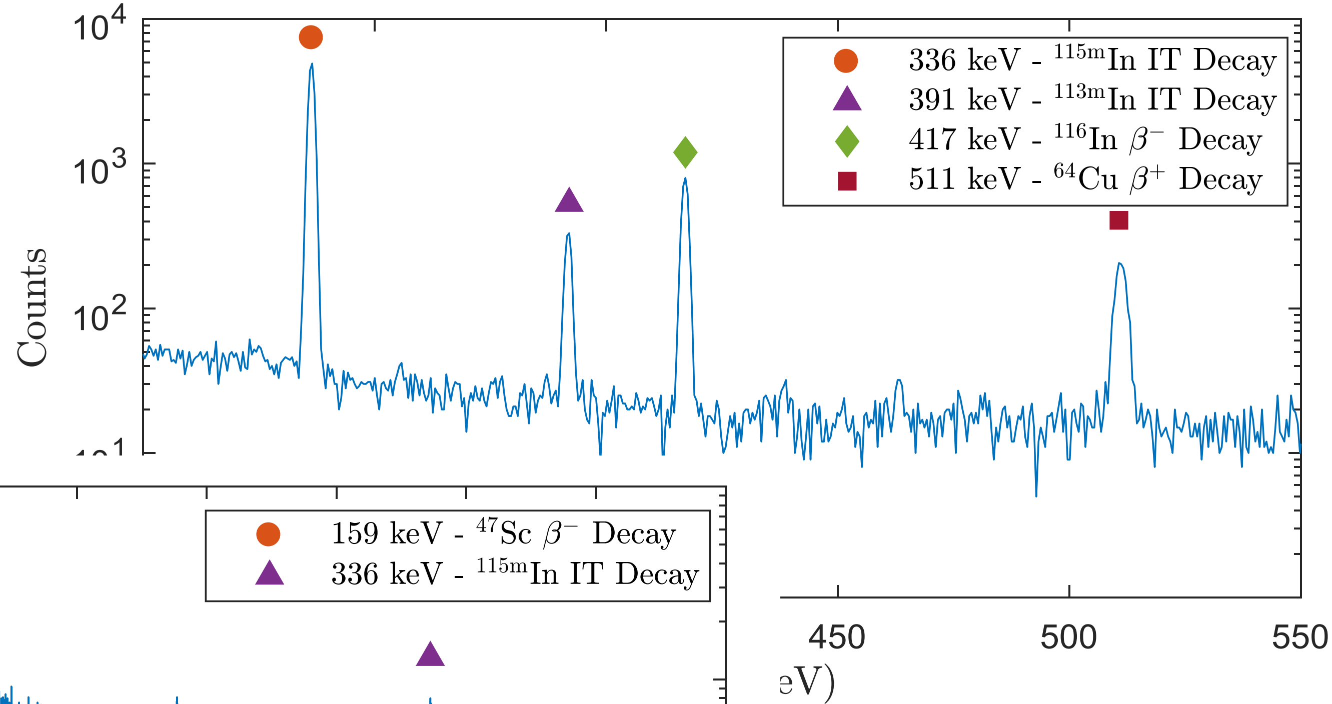

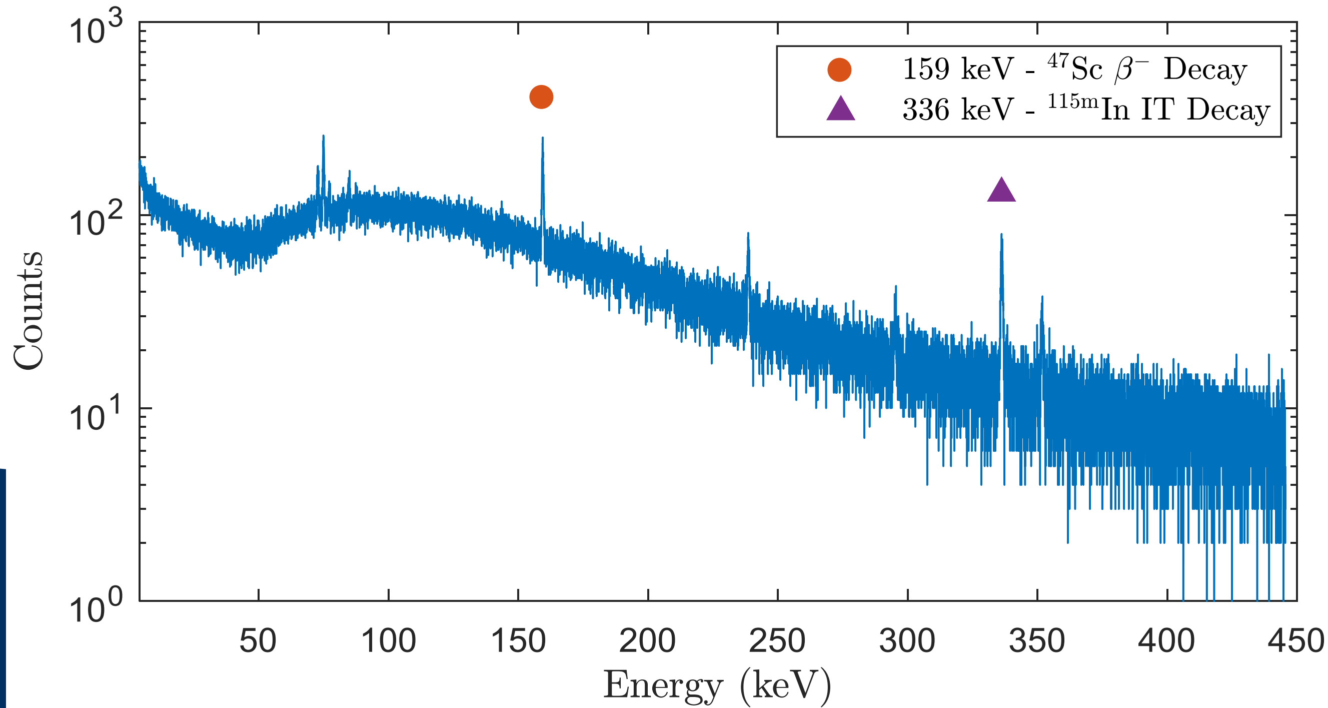

Relative Activation Measurements

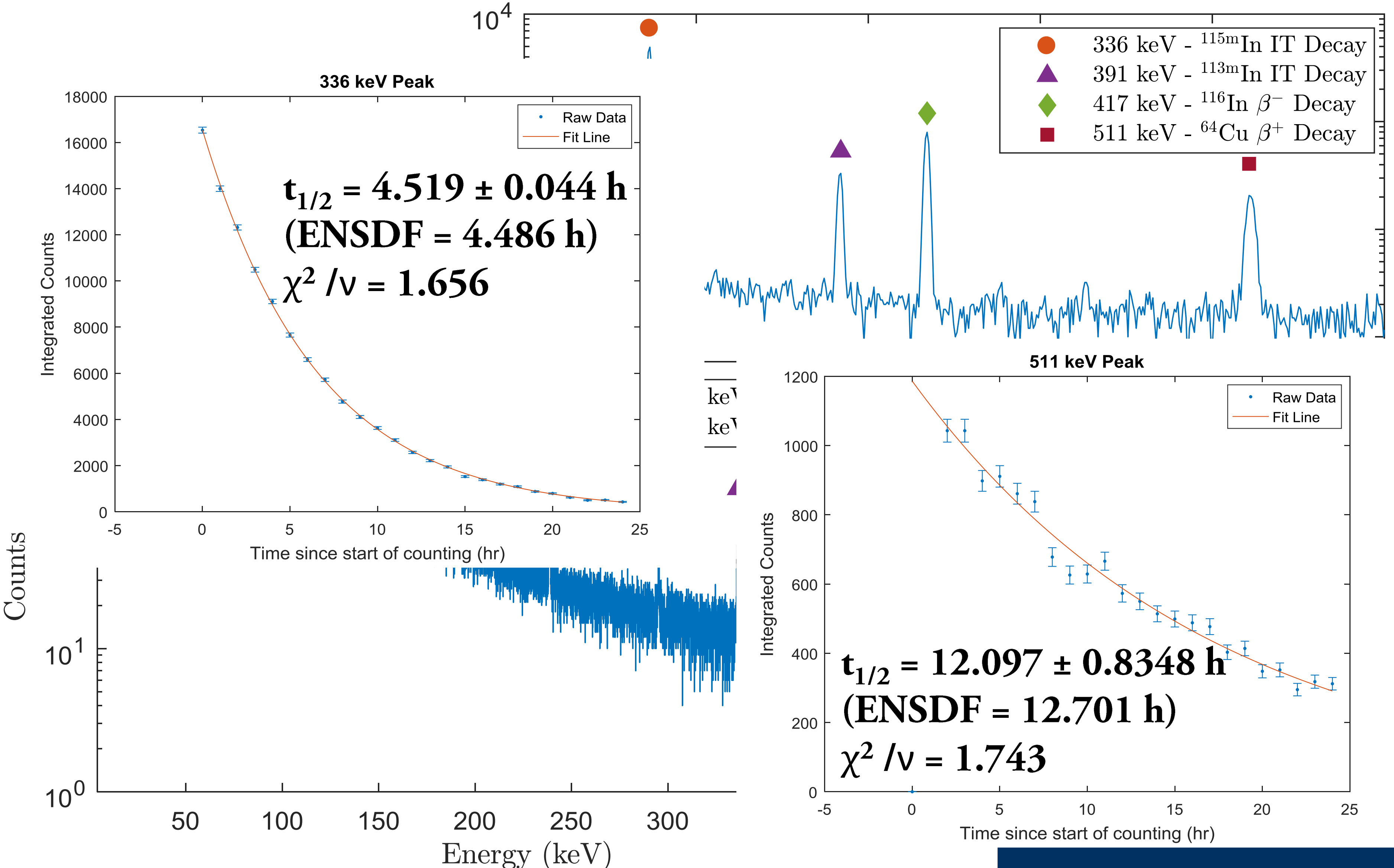

Relative Activation Measurements

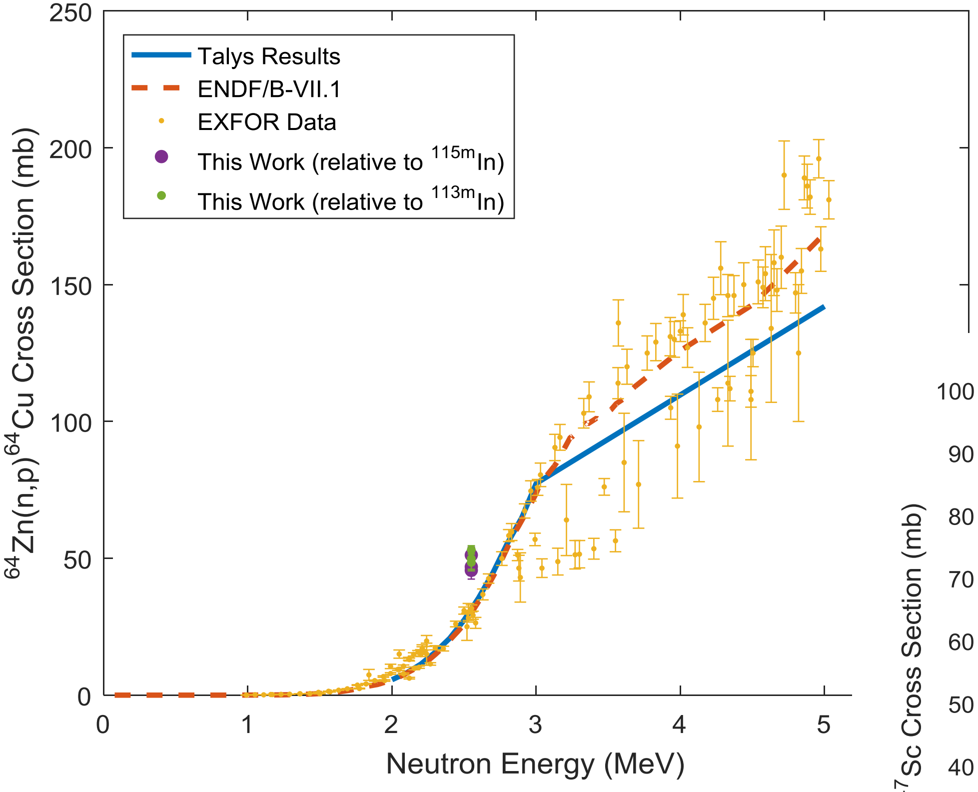

What's going on???

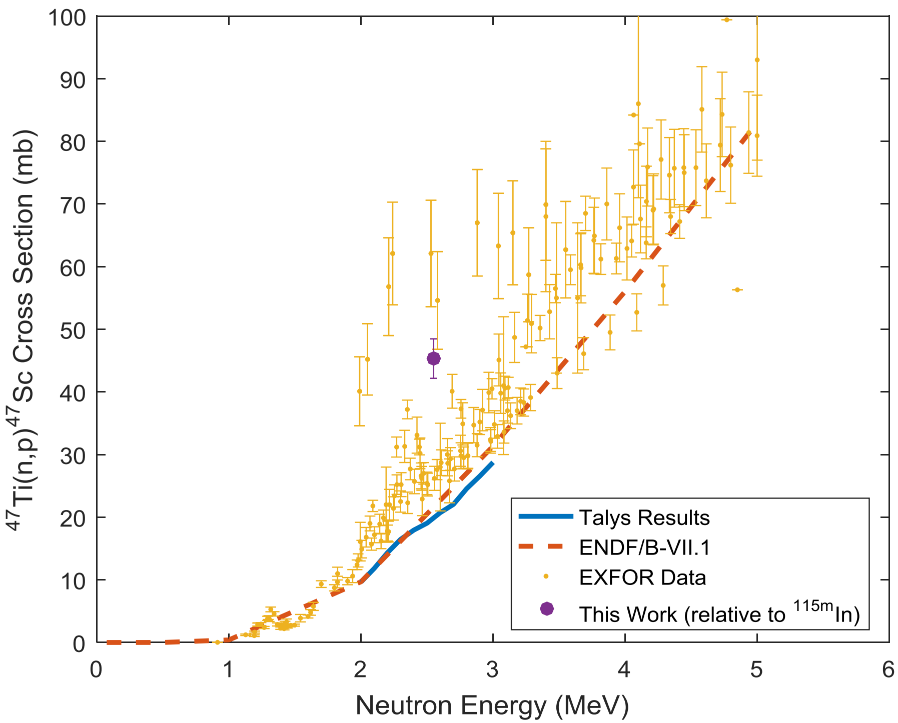

Berkeley
UNIVERSITY OF CALIFORNIA

Neutron Energy Spread

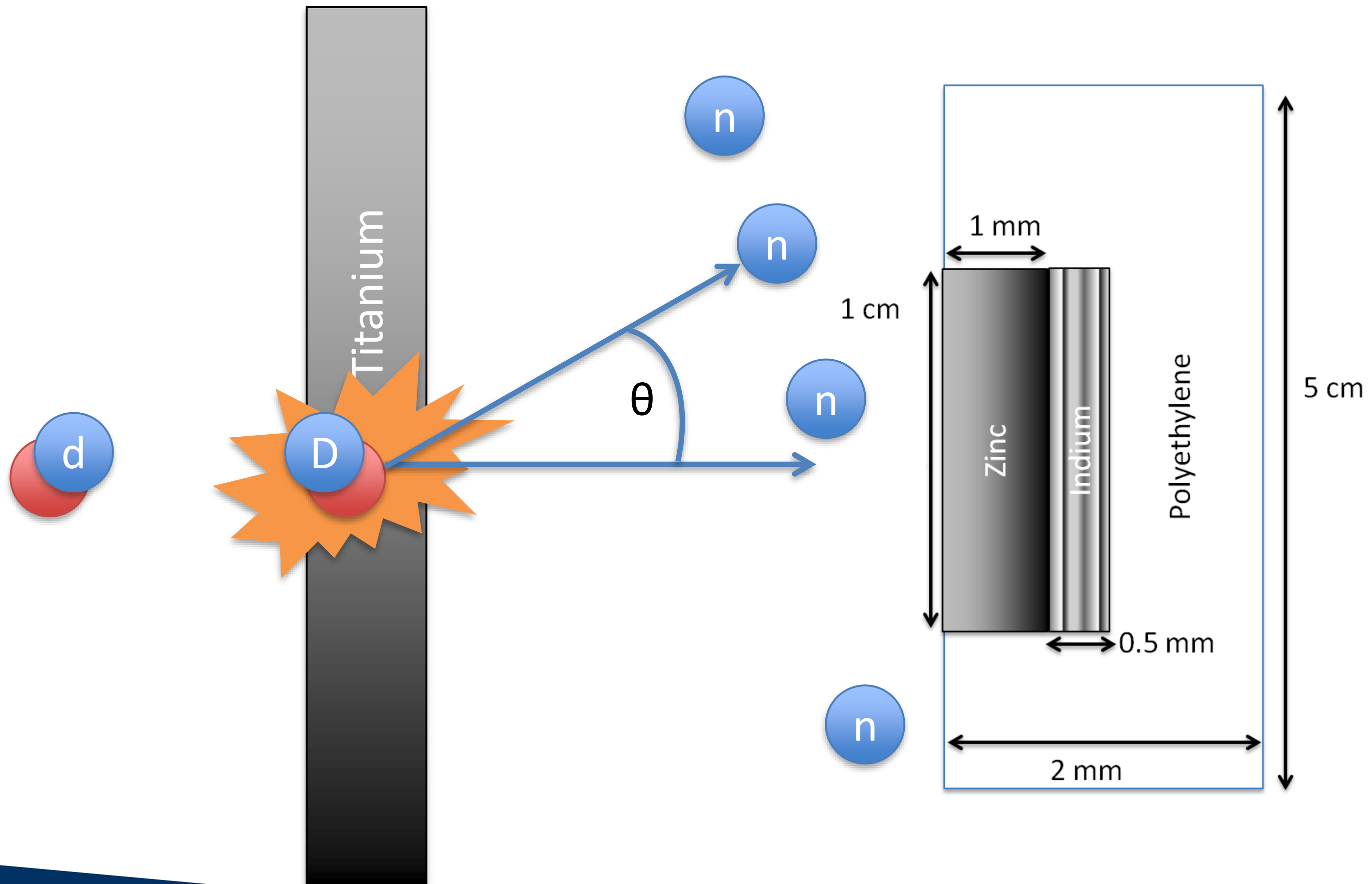

Neutron Energy Spread

H. Liskien *et al.*, Nucl Data Tables, vol 11, 2973

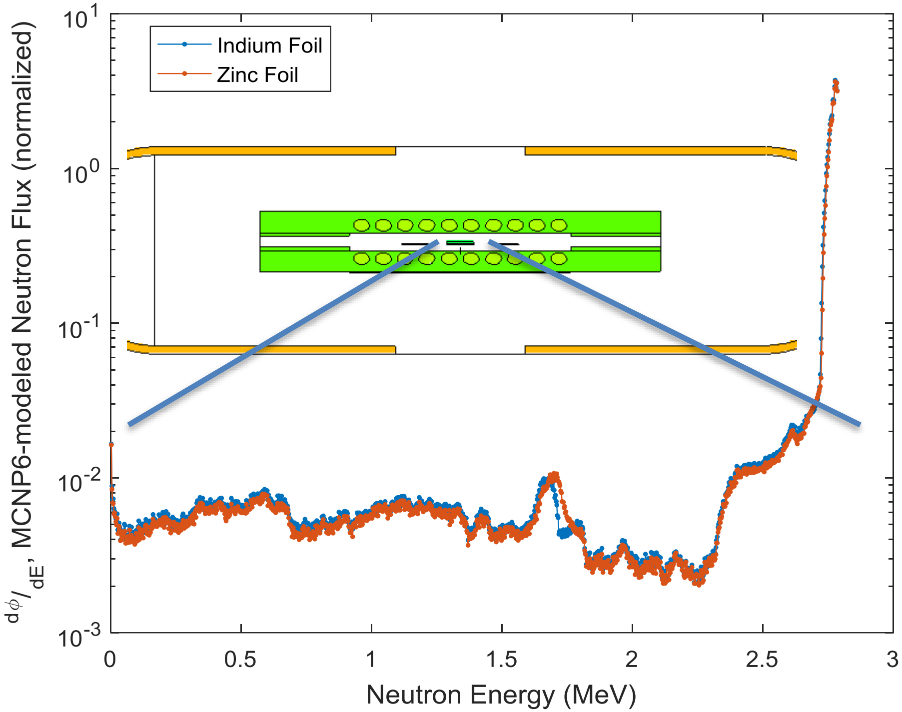

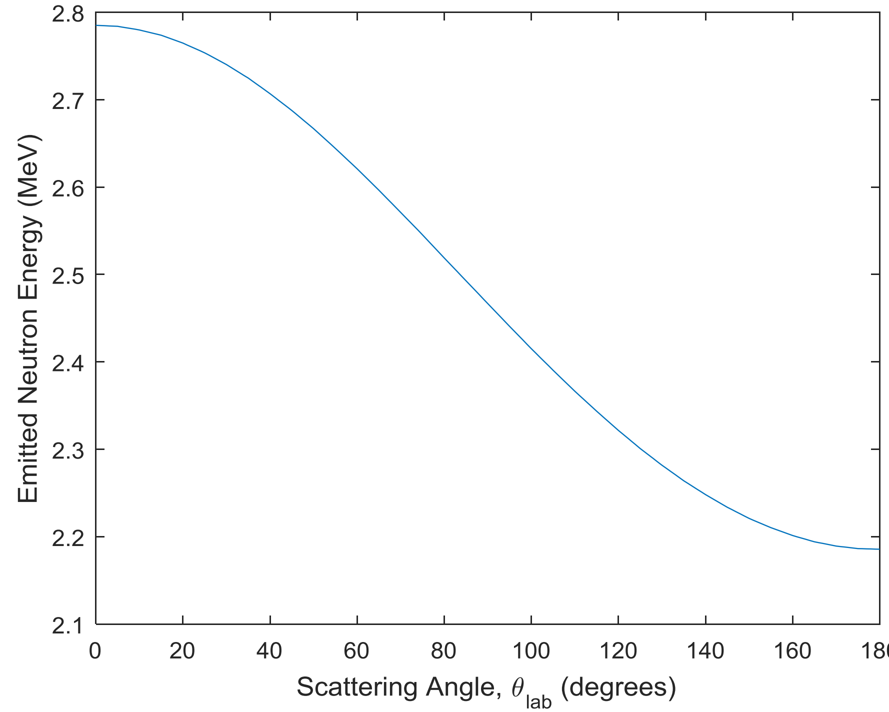

Neutron flux profile modeled in target and monitor foil, using MCNP6

Neutron Energy Spread

H. Liskien *et al.*, Nucl Data Tables, vol 11, 2973

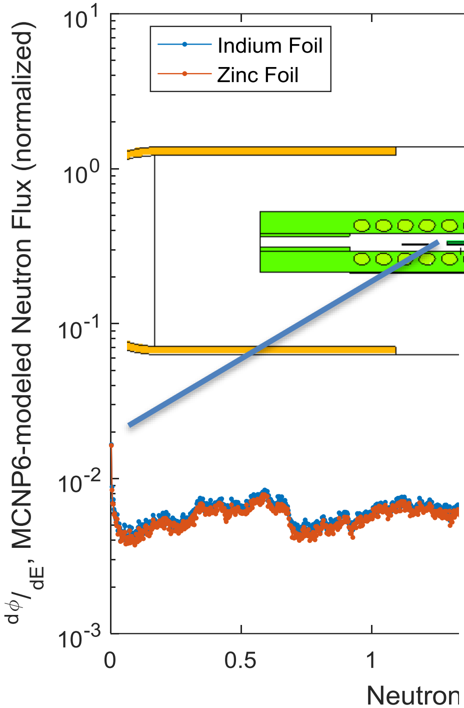

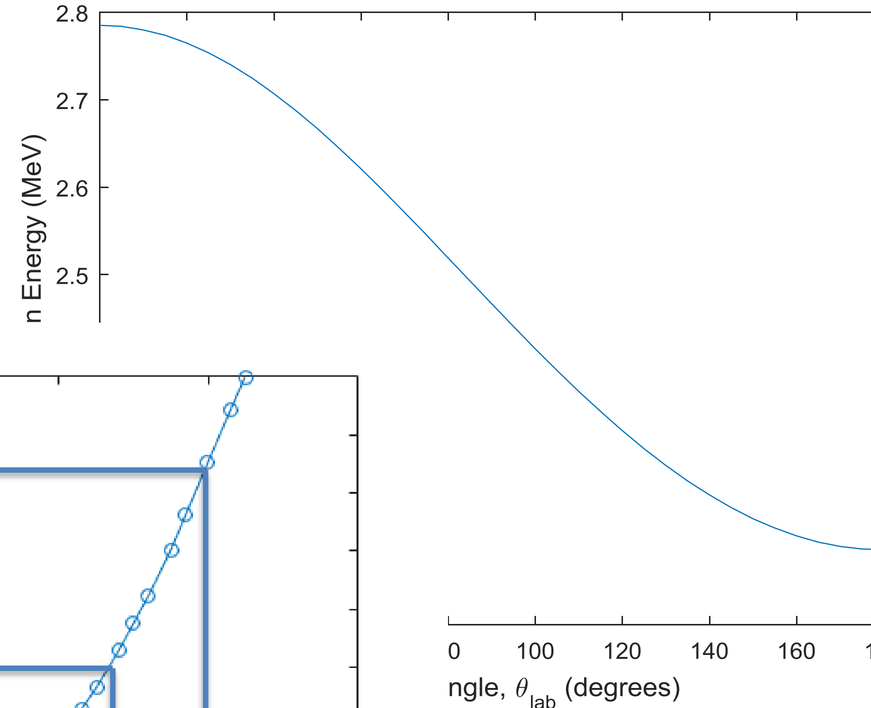

Neutron flux in target and using MCNP6

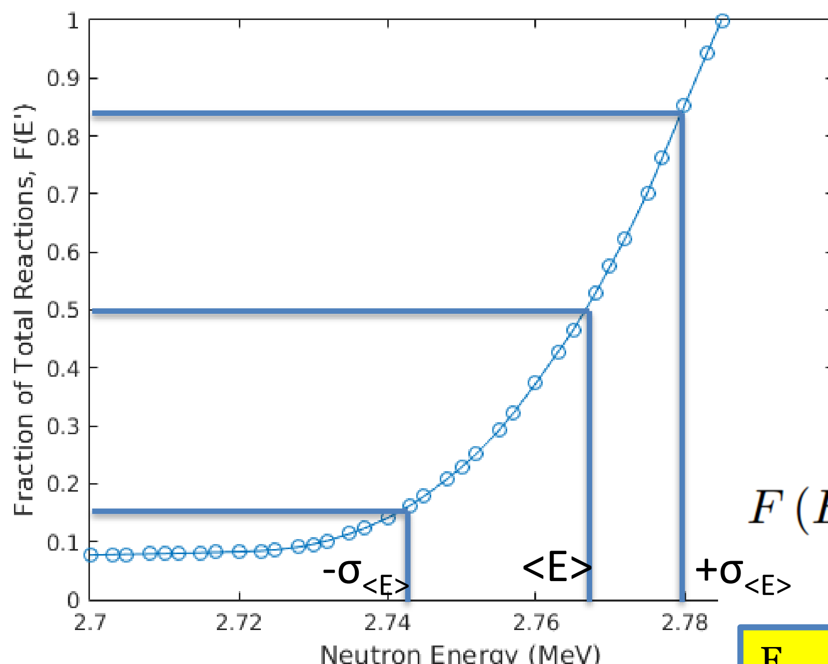

$$F(E') = \frac{\int_0^{E'} \sigma(E) \frac{d\phi}{dE} dE}{\int_0^{E_{max}} \sigma(E) \frac{d\phi}{dE} dE}$$

E_{max} = Maximum energy neutron subtended by foil
F(E') = Fraction of Total Reactions induced up to energy E'

Neutron Energy Spread

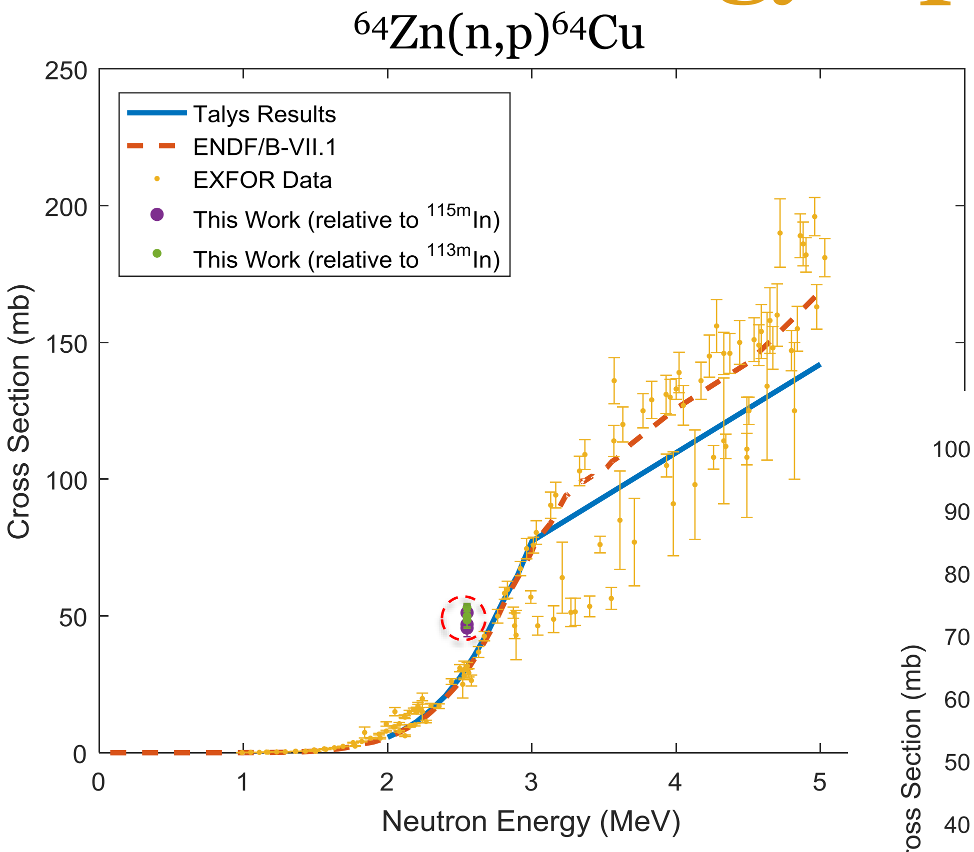

Before…

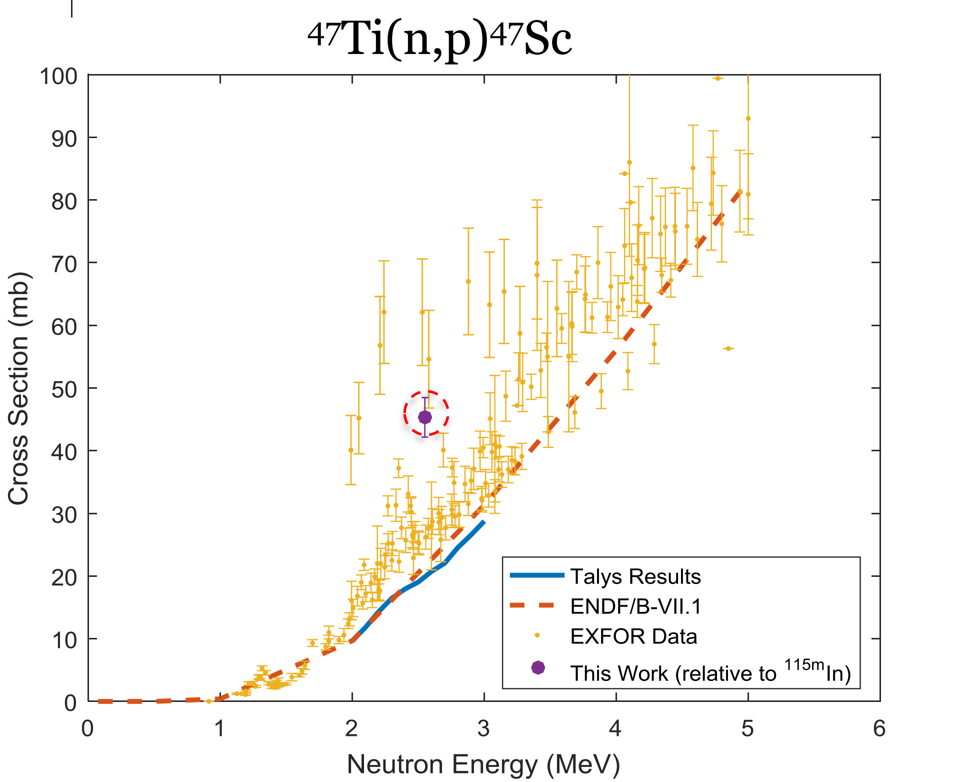

Berkeley
UNIVERSITY OF CALIFORNIA

Neutron Energy Spread

Table 3. Results of cross section measurement.

Reaction	$\sigma(E_n = 2.7645$ MeV) (mb)
^{64}Zn(n,p)^{64}Cu (relative to ^{113}In)	45.953 ± 3.351, 46.493 ± 2.805, 46.9 ± 3.189
^{64}Zn(n,p)^{64}Cu (relative to ^{115}In)	49.716 ± 3.335, 49.011 ± 2.698,
^{47}Ti(n,p)^{47}Sc (relative to ^{115}In)	25.901 ± 1.7089,

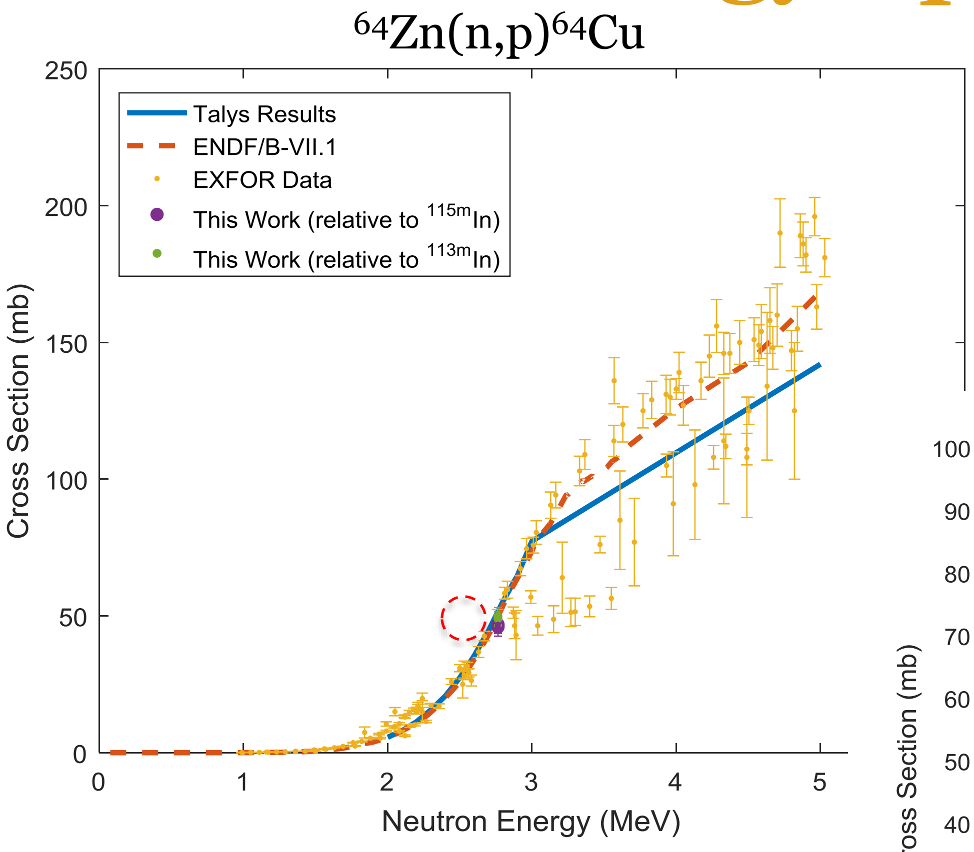

After!

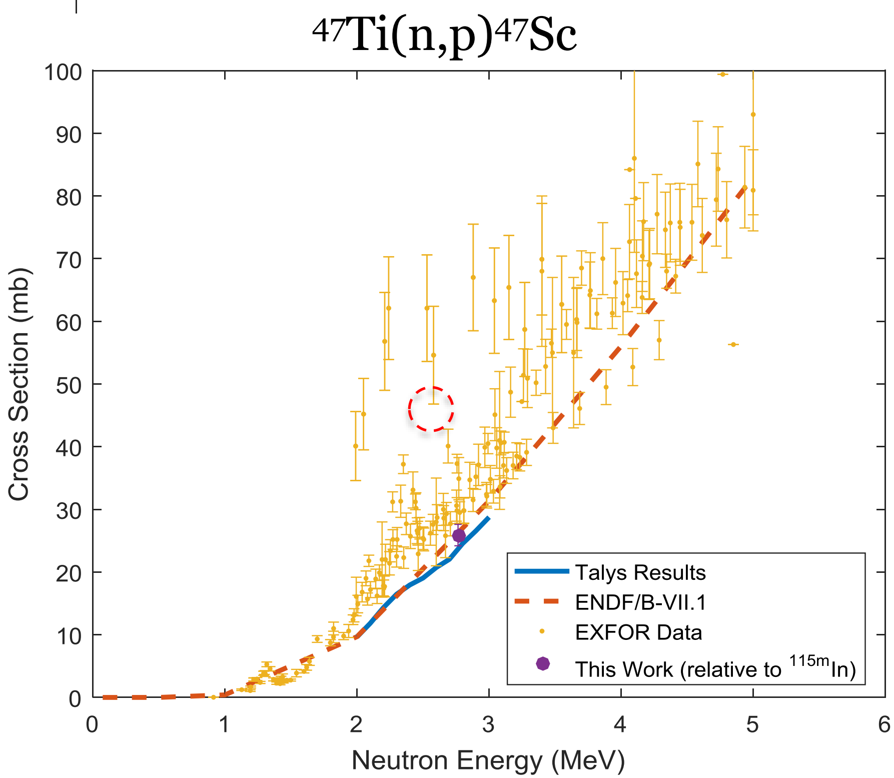

Neutron Energy Spread

Table 3. Results of cross section measurement.

Reaction	$\sigma(E_n = 2.7645$ MeV) (mb)
^{64}Zn(n,p)^{64}Cu (relative to ^{113}In)	45.953 ± 3.351, 46.493 ± 2.805, 46.9 ± 3.189
^{64}Zn(n,p)^{64}Cu (relative to ^{115}In)	49.716 ± 3.335, 49.011 ± 2.698,
^{47}Ti(n,p)^{47}Sc (relative to ^{115}In)	25.901 ± 1.7089,

^{64}Zn(n,p)^{64}Cu

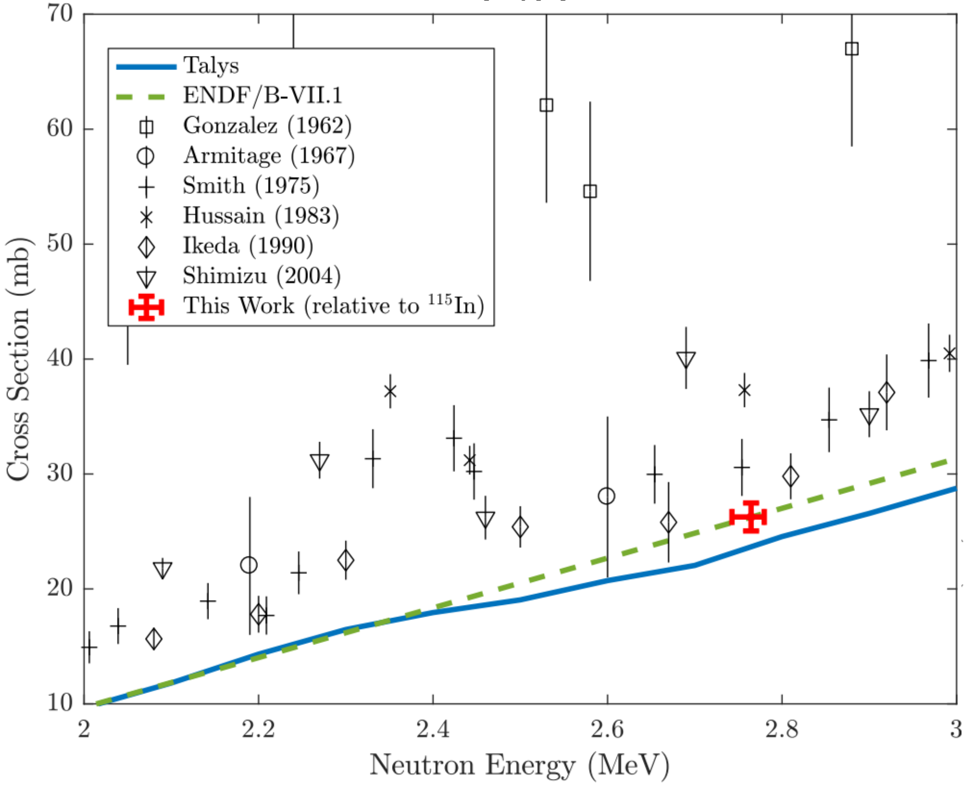

After!

^{47}Ti(n,p)^{47}Sc

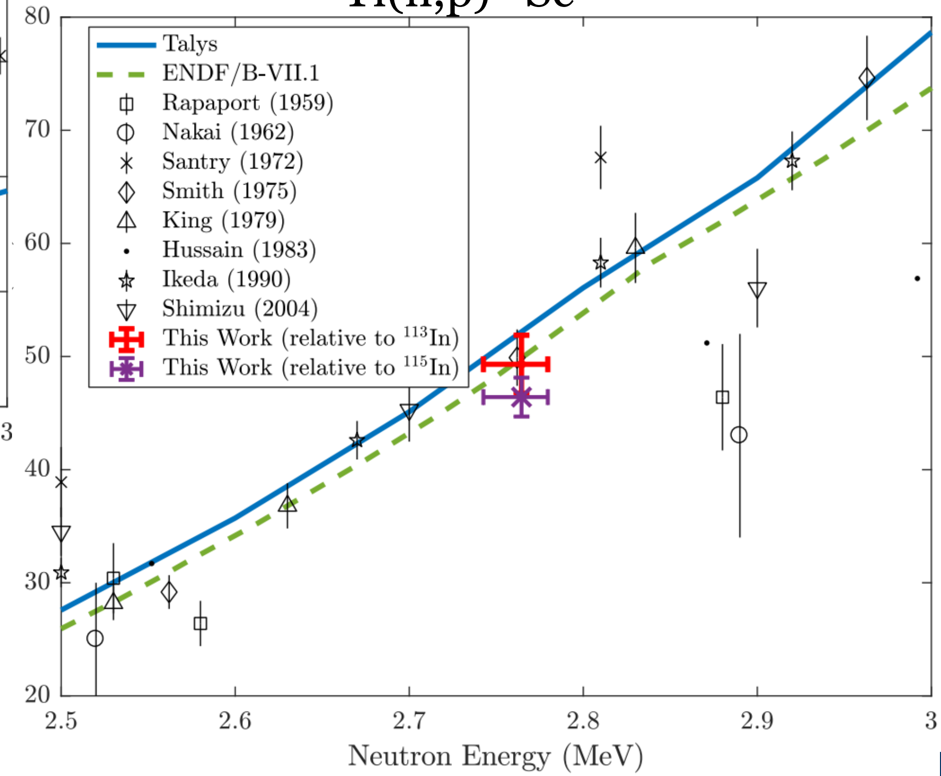

Future Work

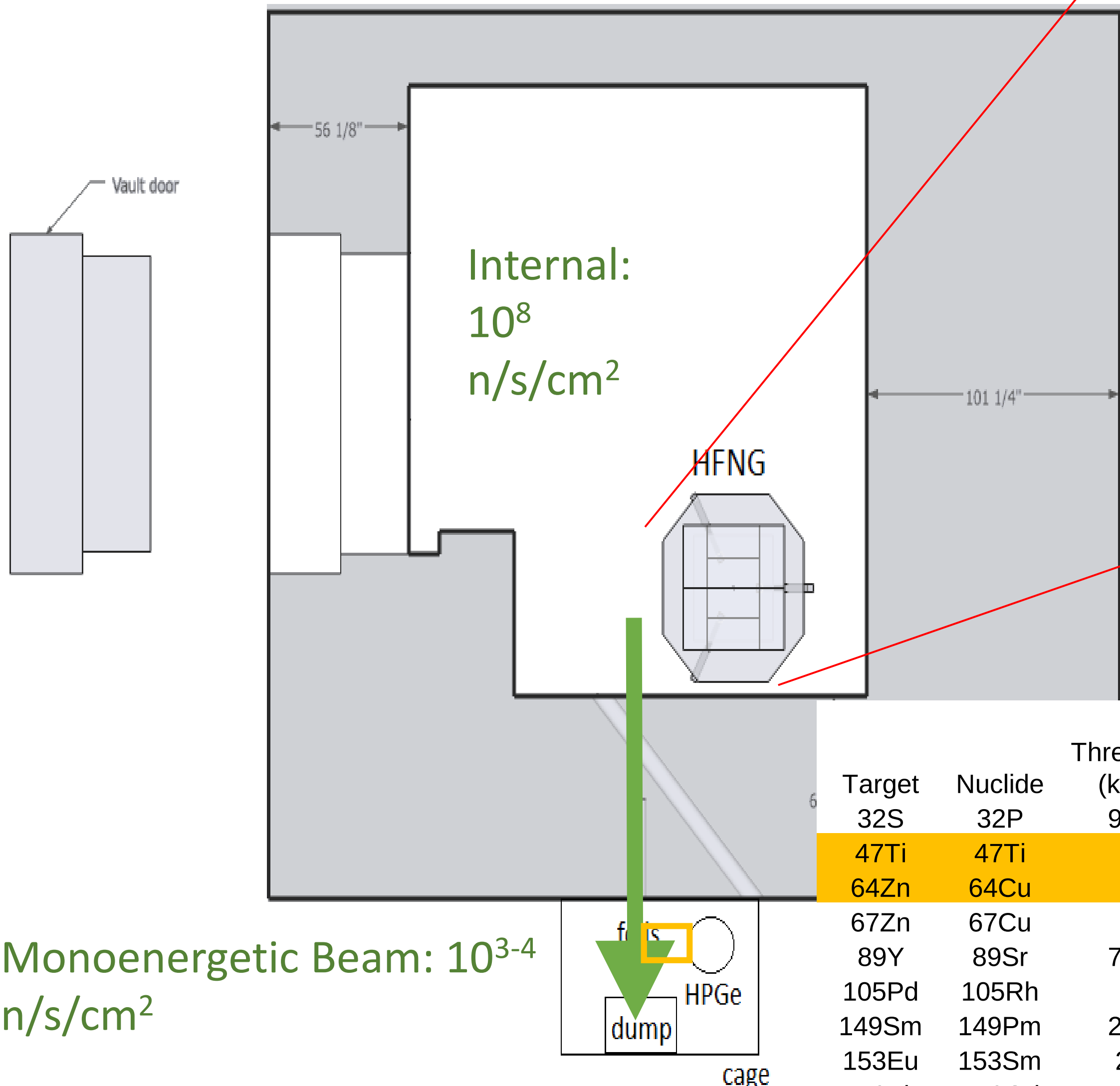

Monoenergetic Beam: $10^{3\text{-}4}$ n/s/cm^2

Phase 1 current upgrade complete!

Target	Nuclide	Threshold (keV)	% abundance	Strongest γ-ray branch (keV)	# seen in a 0.5% Ge detector	Rate in a 0.5% detector
32S	32P	985	95%	0	0.00E+00	0.00
47Ti	47Ti	0	7.44%	159.381	1.24E+05	1.44
64Zn	64Cu	0	49.20%	511	5.03E+05	5.82
67Zn	67Cu	0	4.04%	184.577	5.45E+04	0.63
89Y	89Sr	726	100%	908.96	1.25E+02	0.00
105Pd	105Rh	0	22.33%	318.9	1.27E+05	1.47
149Sm	149Pm	291	11.24%	285.94	4.47E+03	0.05
153Eu	153Sm	25	52.19%	103.18	1.36E+05	1.58
159Tb	159Gd	190	100%	363.543	1.58E+05	1.83
161Dy	161Tb	0	18.89%	75.57	2.66E+04	0.31
166Er	166Ho	1079	33.50%	1379.4	4.39E+03	0.05
169Tm	169Er	0	100%	109.8	1.87E+01	0.00
175Lu	175Yb	0	97.40%	396.3	1.88E+05	2.18
177Hf	177Lu	0	18.60%	208.4	3.77E+04	0.44

Berkeley
UNIVERSITY OF CALIFORNIA

Stacked-target Charged Particle Excitation Functions

LBNL / LANL

^{51,52}Mn - Motivation

- Emerging medical radionuclides
  - ^{51}Mn ($t_{1/2}$ = 46 min, 97% β^+) – short-lived PET tracer for metabolic studies
  - ^{52g}Mn ($t_{1/2}$ = 5.6 d, 29% β^+) – long-lived PET tracer for neuron tracking, immune studies

Preparation and *in vivo* characterization of $^{51}MnCl_2$ as PET tracer of Ca^{2+} channel-mediated transport

Stephen A. Graves[1], Reinier Hernandez[1], Hector F. Valdovinos[1], Paul A. Ellison[1], Jonathan W. Engle[1]* Todd E. Barnhart[1], Weibo Cai[1,2,3], Robert J. Nickles[1]*

  - Manganese has well-established biochemistry and uptake via DOTA-based chelation

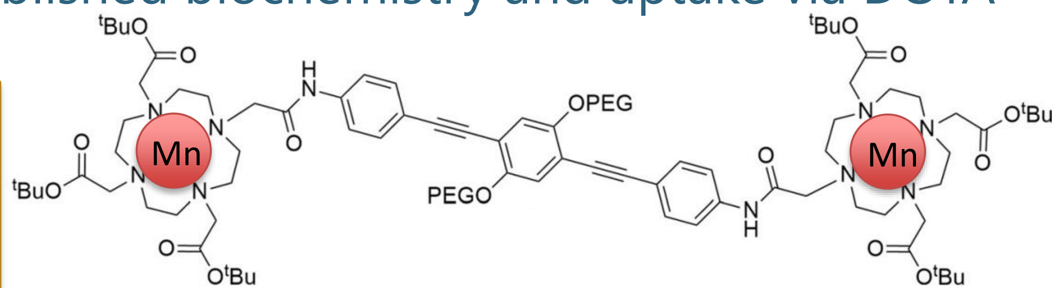

Almost no Fe(p,x) XS measurements exist – can use these to probe spin physics in the A≈50 region

Methodology

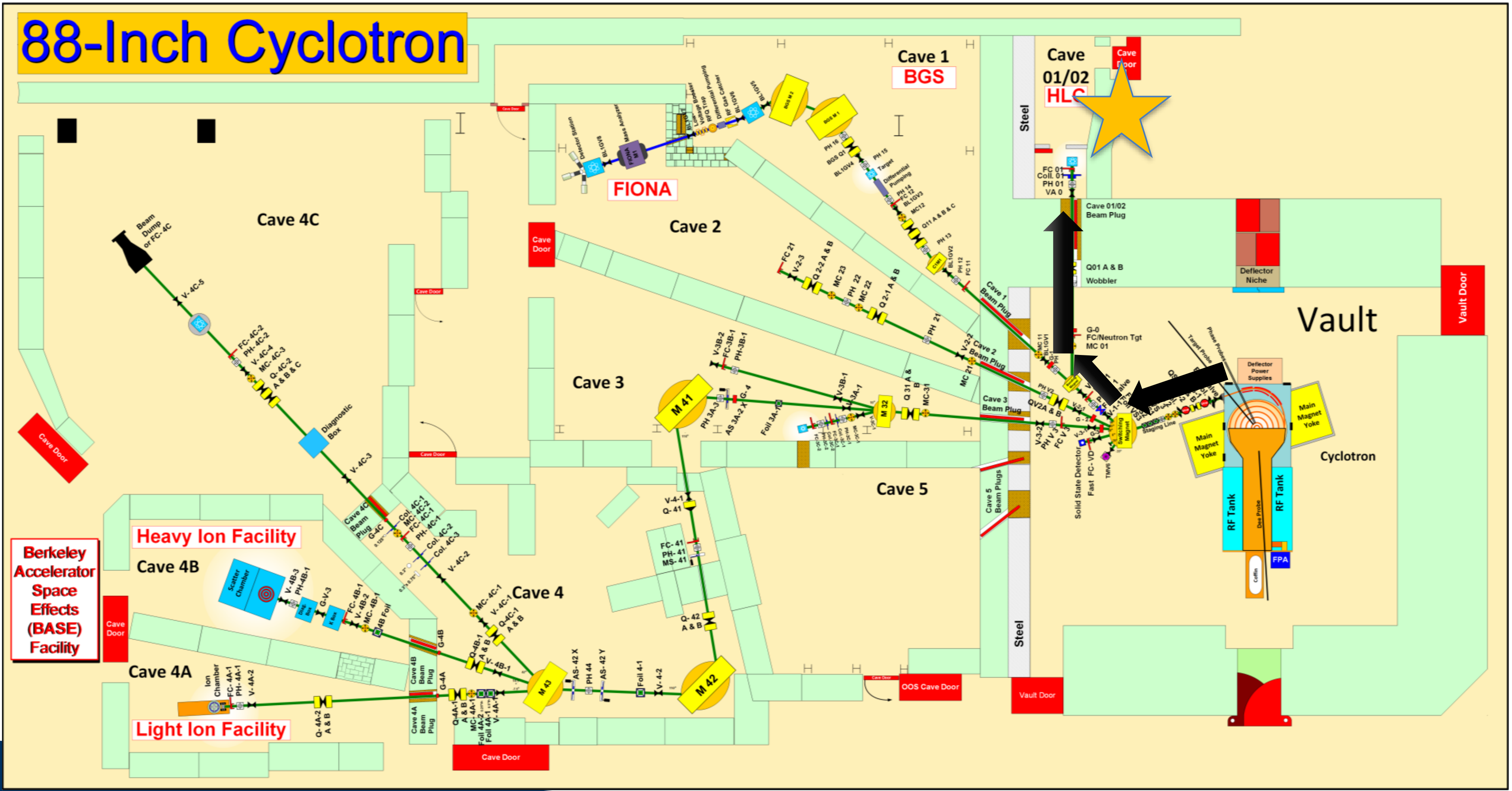

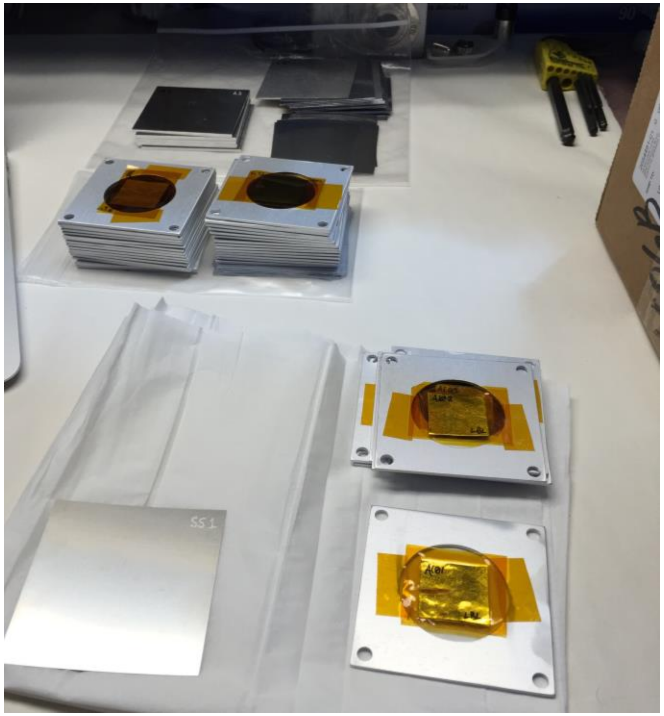

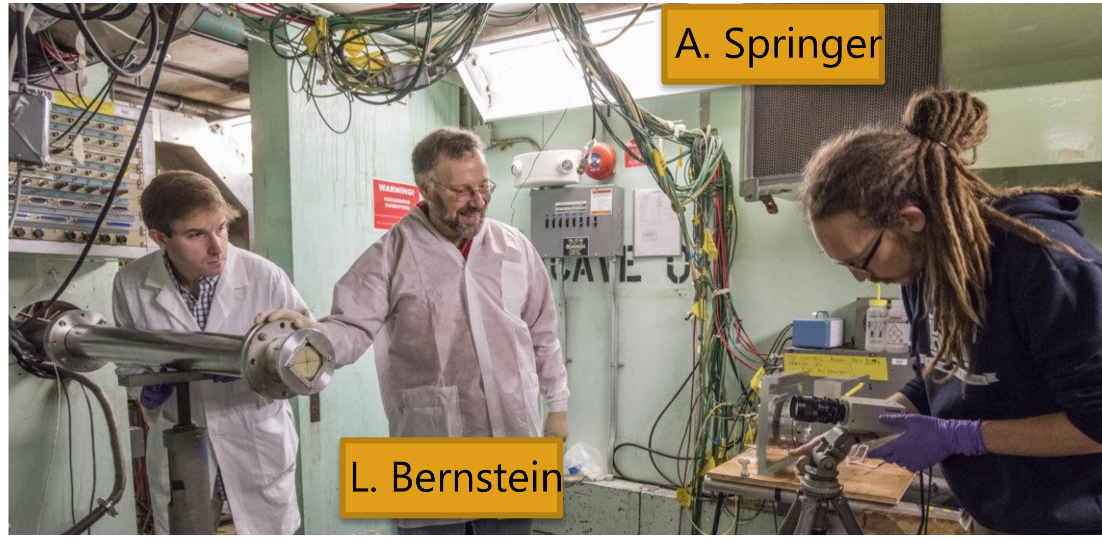

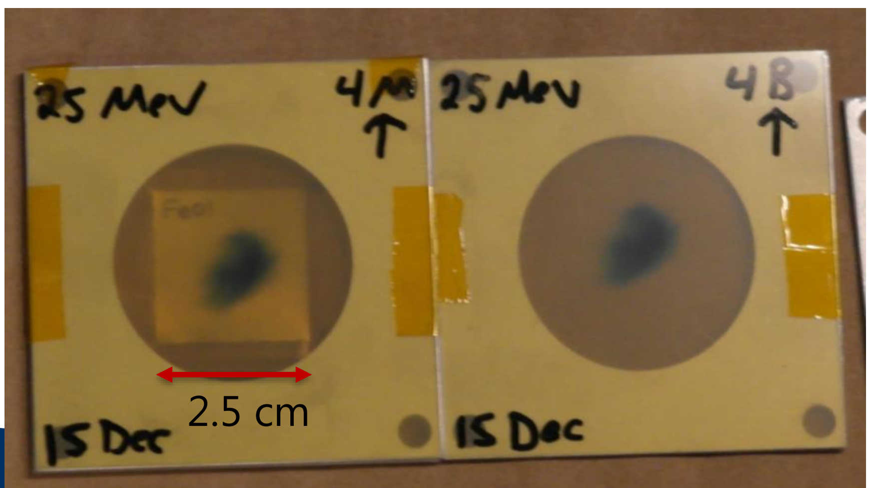

Two overlapping stacks:
E_p= 55→21 MeV, 25→11 MeV

- 25 µm-thin ^{nat}Fe, ^{nat}Cu, ^{nat}Ti foils in 0.1″ Al frames

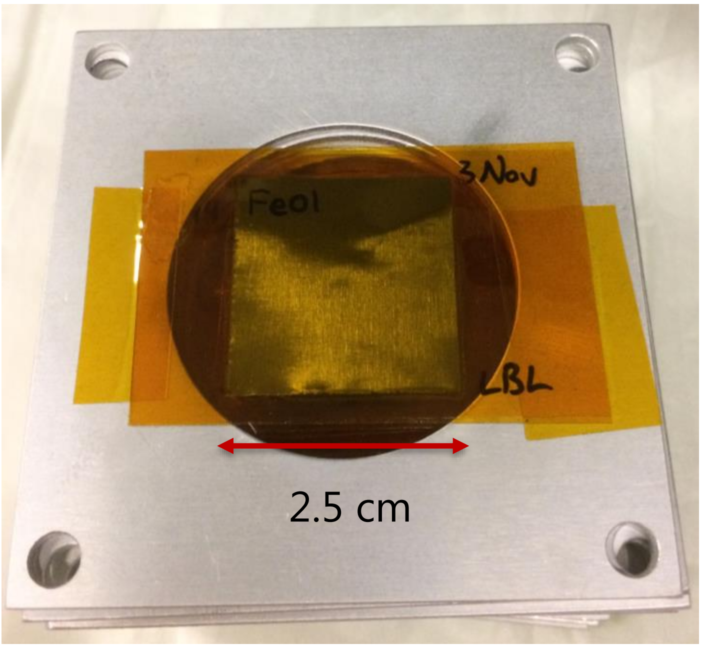

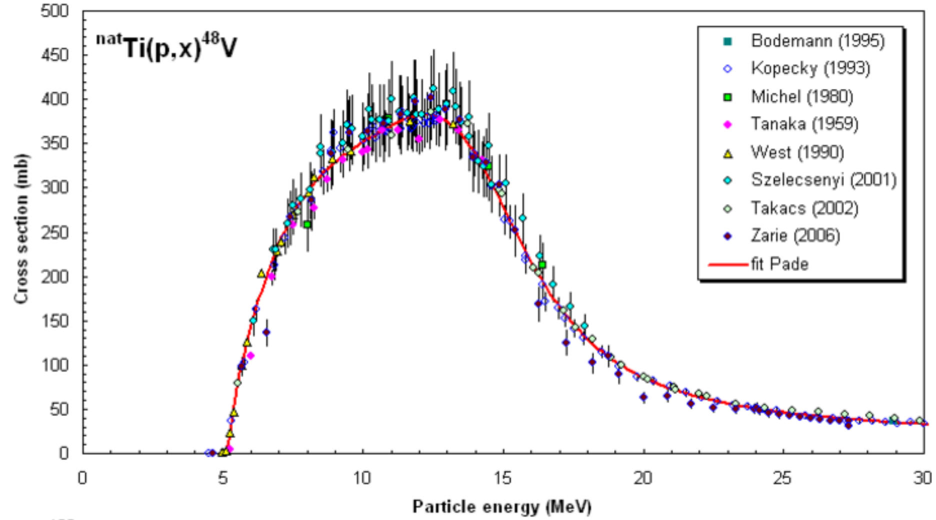

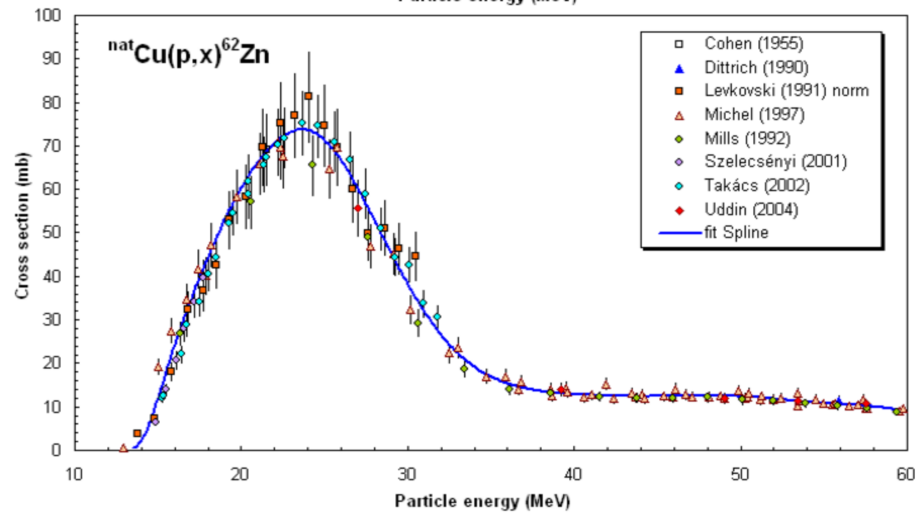

nds.iaea.org/medical/monitor_reactions.html

- Dosimetry: IAEA charged particle beam monitor reactions:
  - $^{nat}Ti(p,x)^{48}V$
  - $^{nat}Cu(p,x)^{62,63,65}Zn$

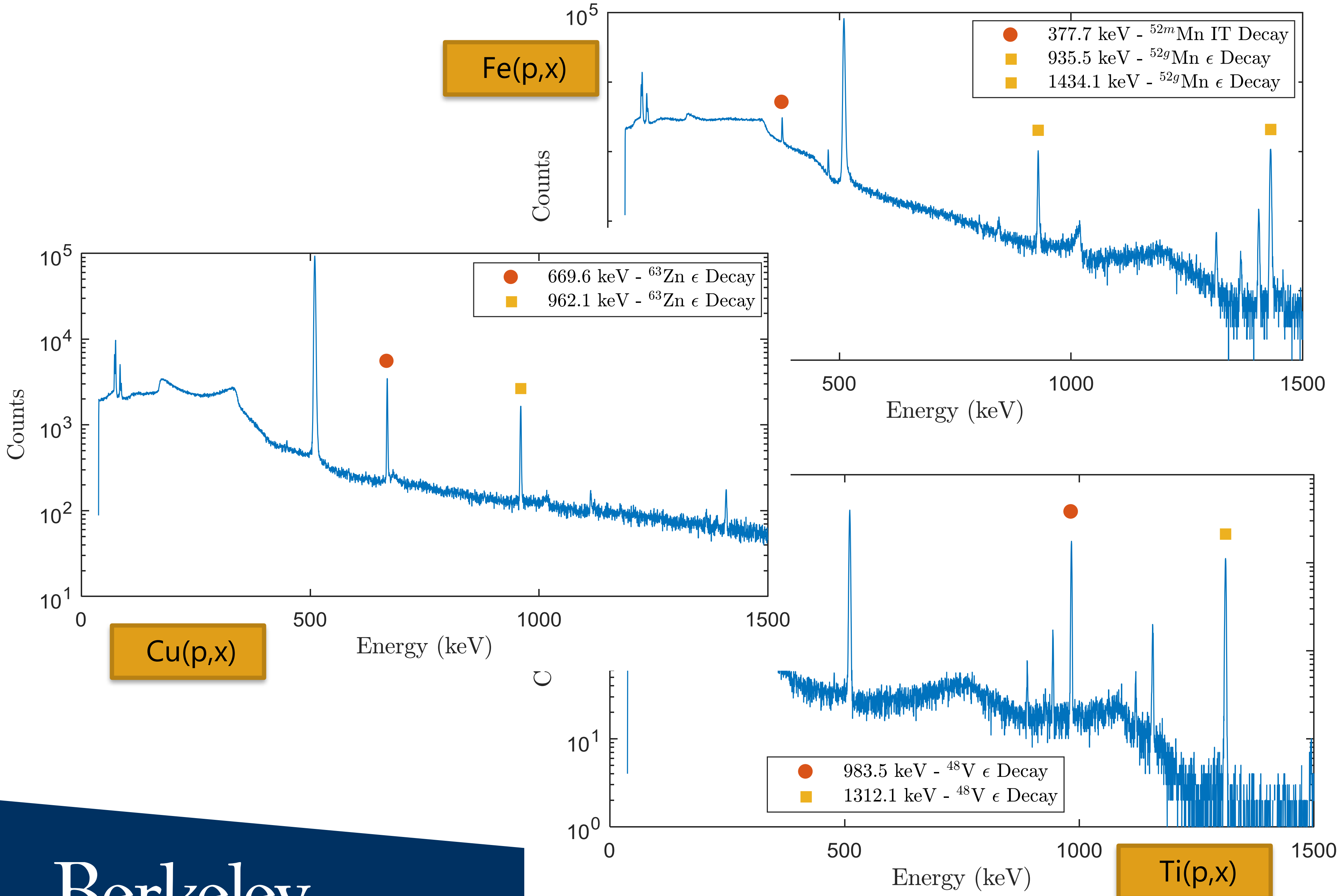
Fe(p,x)
377.7 keV - ^{52m}Mn IT Decay
935.5 keV - ^{52g}Mn ϵ Decay
1434.1 keV - ^{52g}Mn ϵ Decay
Counts
Energy (keV)
Cu(p,x)
669.6 keV - ^{63}Zn ϵ Decay
962.1 keV - ^{63}Zn ϵ Decay
Ti(p,x)
983.5 keV - ^{48}V ϵ Decay
1312.1 keV - ^{48}V ϵ Decay

0.5% initial beam dispersion

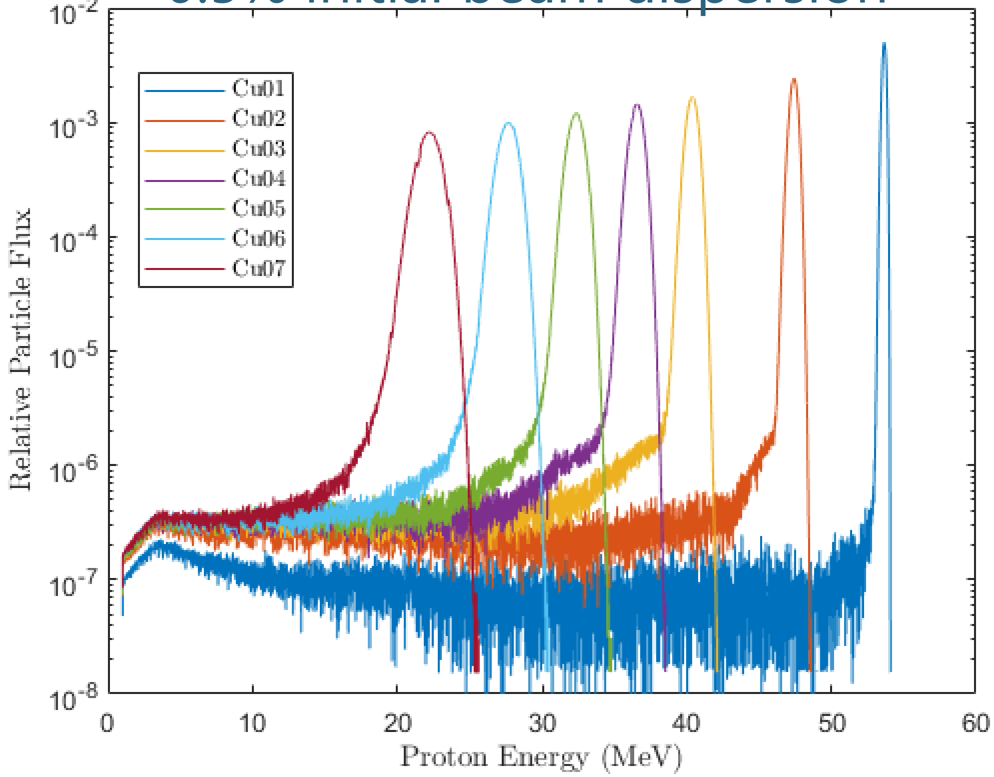

2% initial beam dispersion

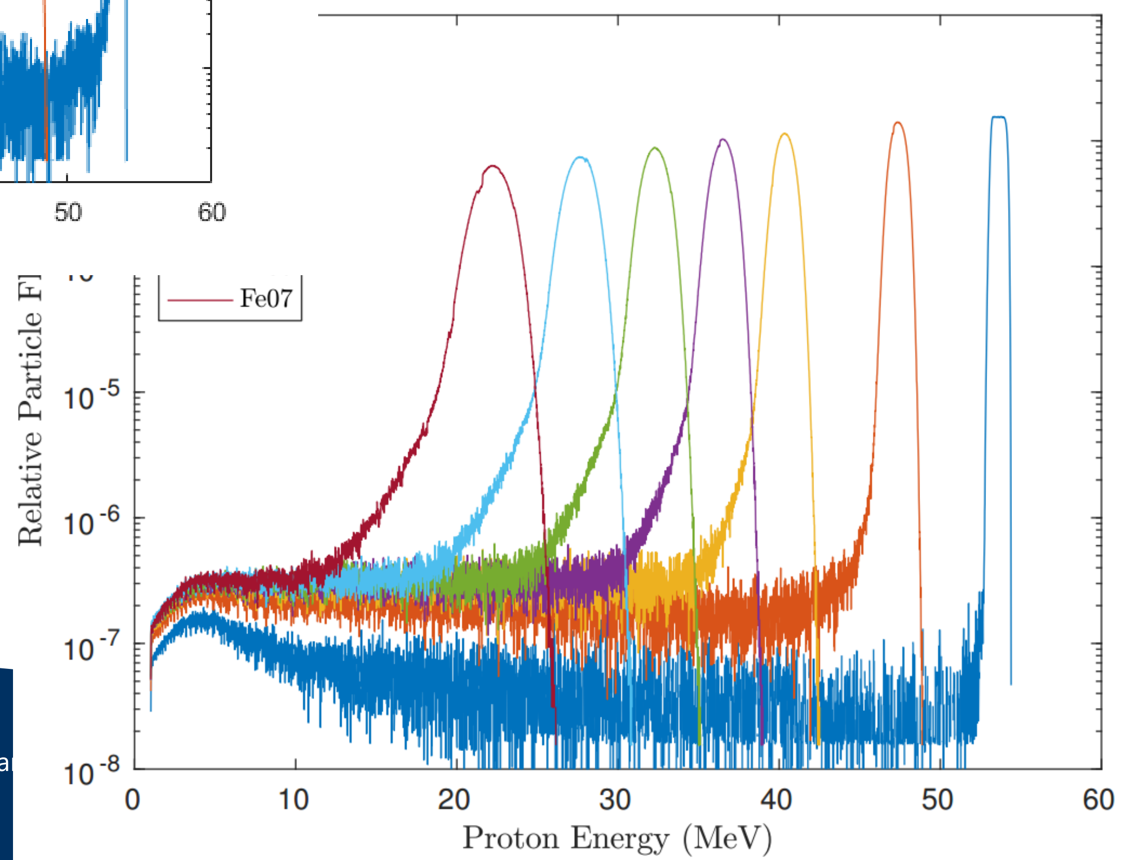

0.5% initial beam dispersion

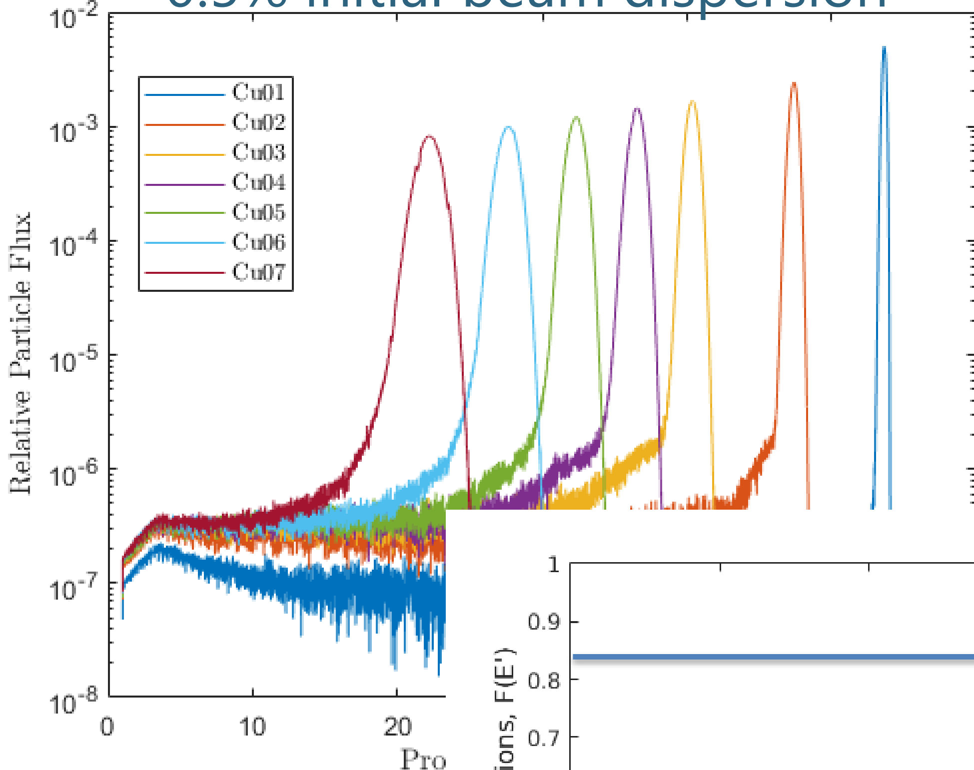

2% initial beam dispersion

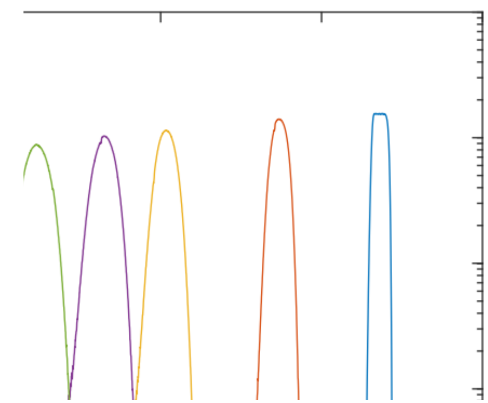

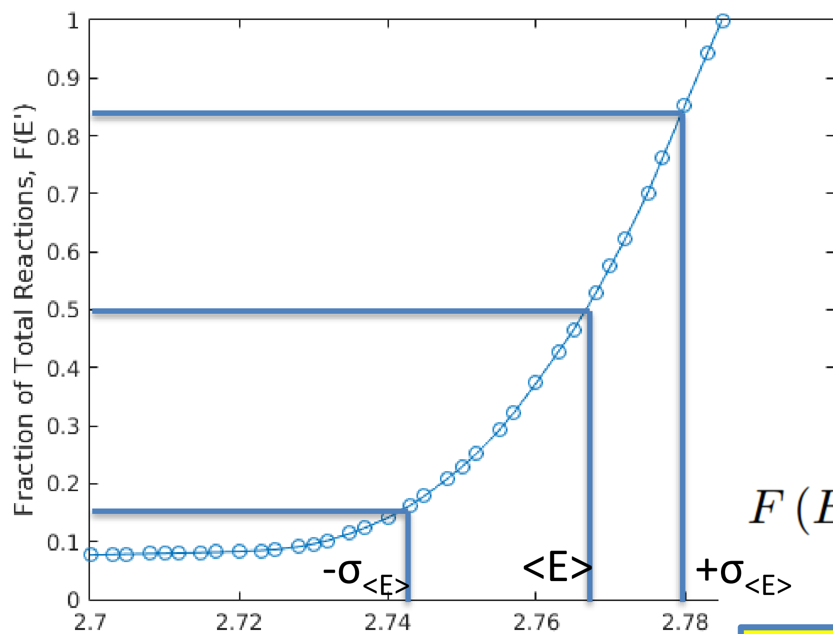

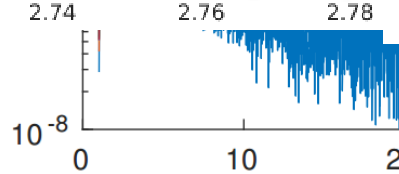

$$F\left(E'\right) = \frac{\int_0^{E'} \sigma(E)\frac{d\phi}{dE}dE}{\int_0^{E_{max}} \sigma(E)\frac{d\phi}{dE}dE}$$

E_{max} = Maximum energy proton subtended by foil
F(E’) = Fraction of Total Reactions induced up to energy E’

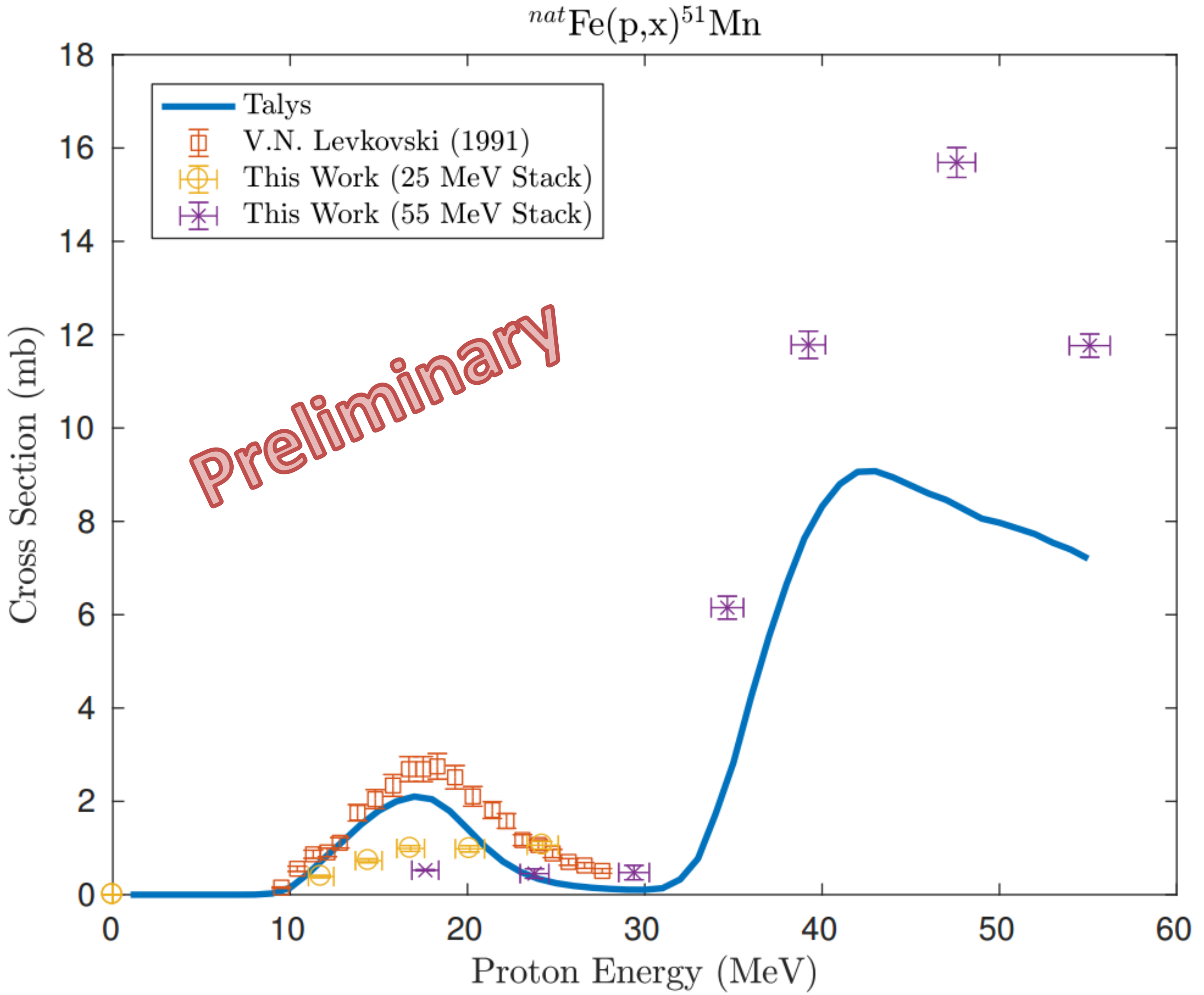
^{nat}Fe(p,x)^{51}Mn
Talys
V.N. Levkovski (1991)
This Work (25 MeV Stack)
This Work (55 MeV Stack)
Preliminary
Cross Section (mb)
Proton Energy (MeV)
0
2
4
6
8
10
12
14
16
18
0
10
20
30
40
50
60

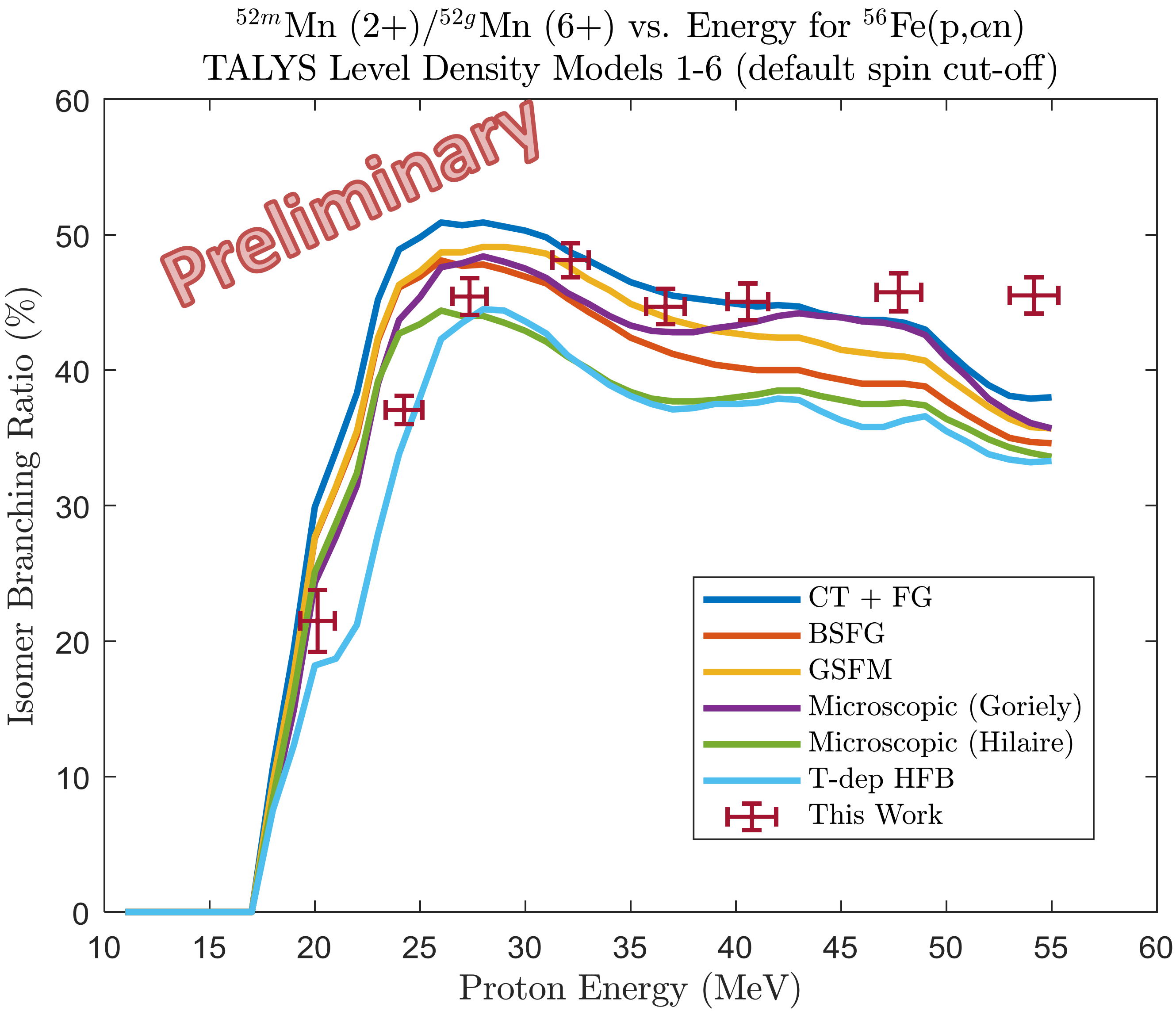
^{52m}Mn (2+)/^{52g}Mn (6+) vs. Energy for ^{56}Fe(p,αn)
TALYS Level Density Models 1-6 (default spin cut-off)
Preliminary
Isomer Branching Ratio (%)
Proton Energy (MeV)
0
10
20
30
40
50
60
10
15
20
25
30
35
40
45
50
55
60
CT + FG
BSFG
GSFM
Microscopic (Goriely)
Microscopic (Hilaire)
T-dep HFB
This Work

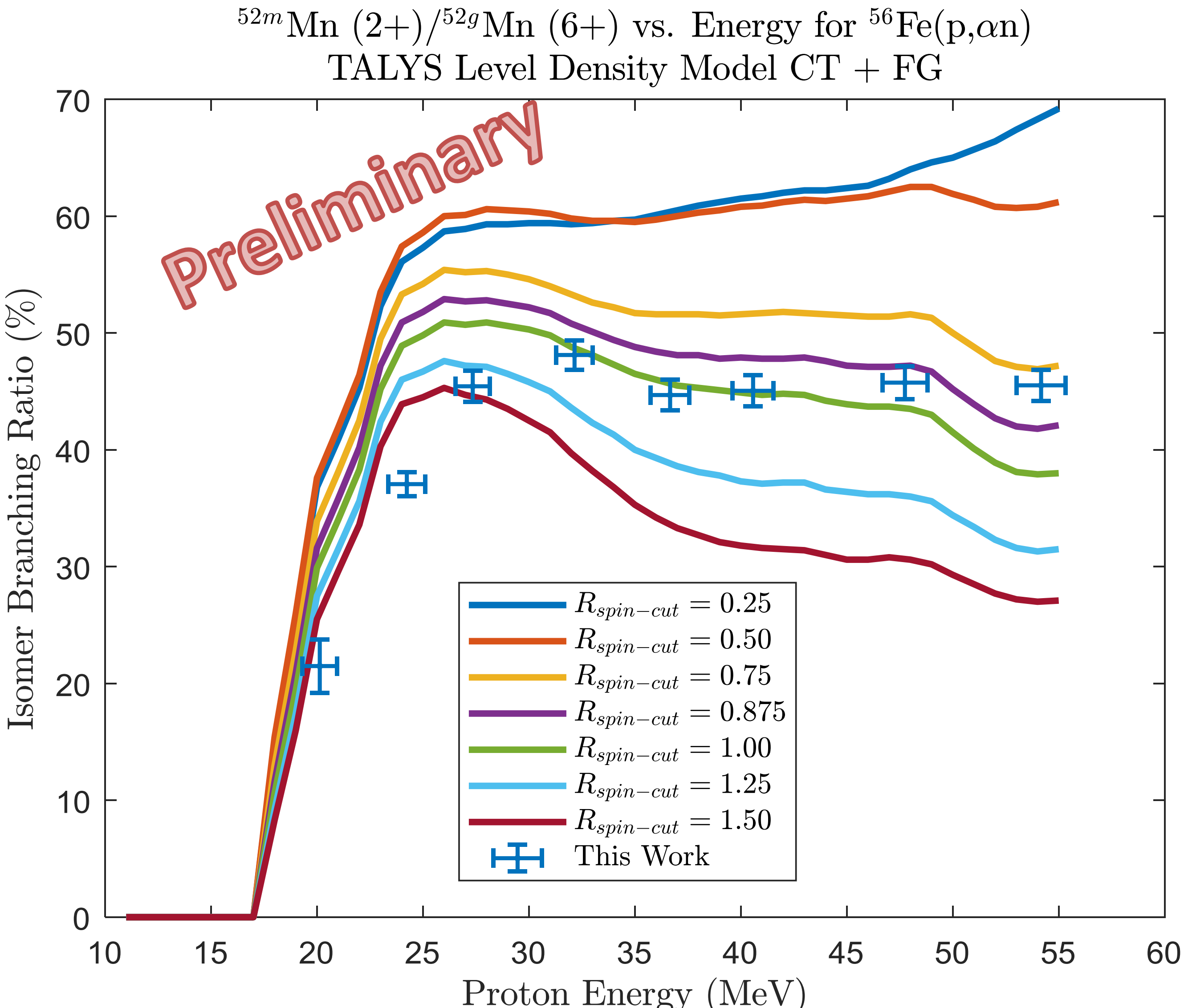

Results consistent with R≈1 at high energy.

At low energy, results are ambiguous due to energy straggling.

Measurements @ LANL – Nb(p,x)

- $^{nat}Nb(p,4n)^{90}Mo$ is a high-priority objective as a new proton beam dosimetry standard for $E_p \approx 50 – 100$ MeV

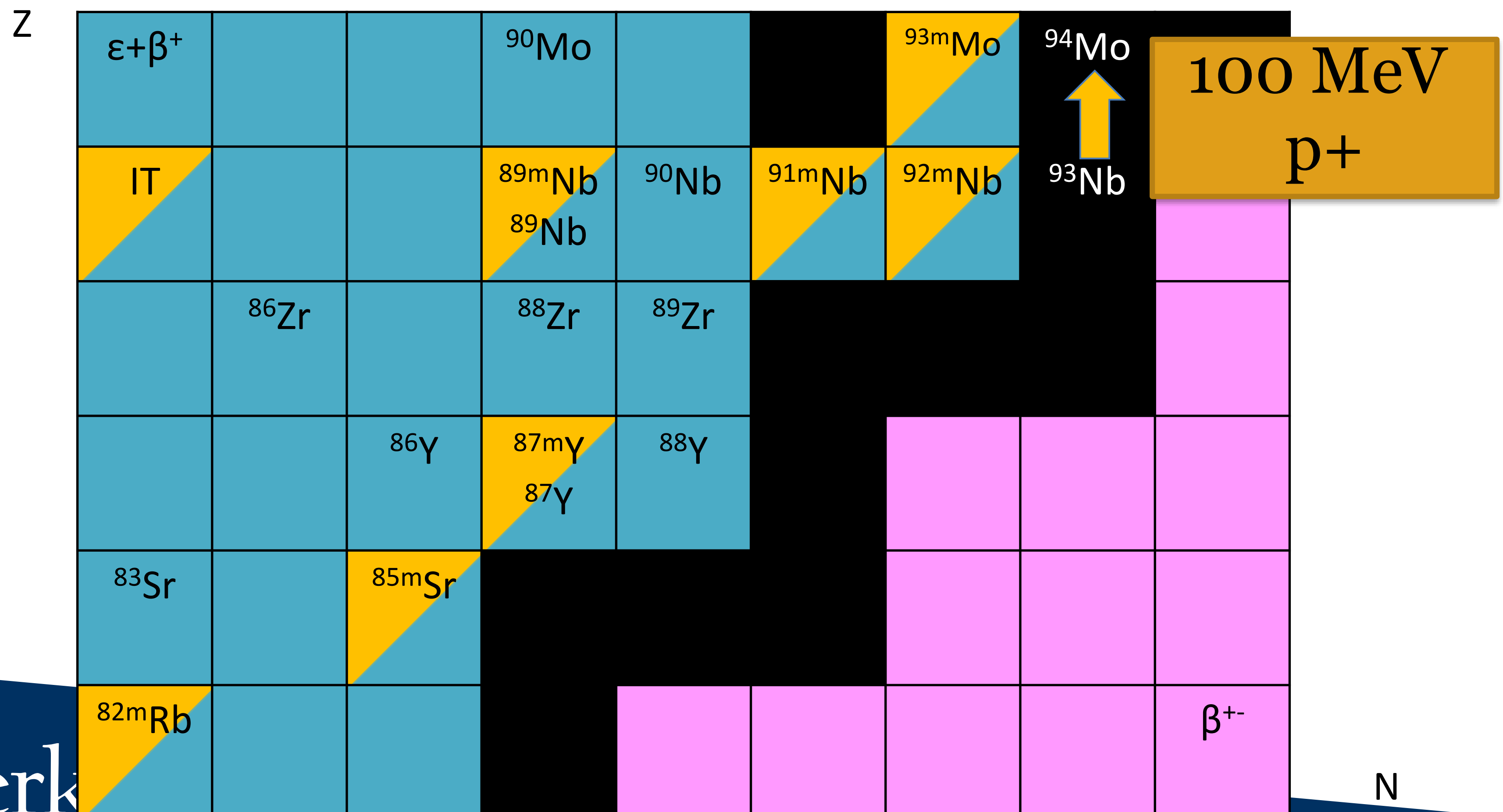

Measurements @ LANL – Nb(p,x)

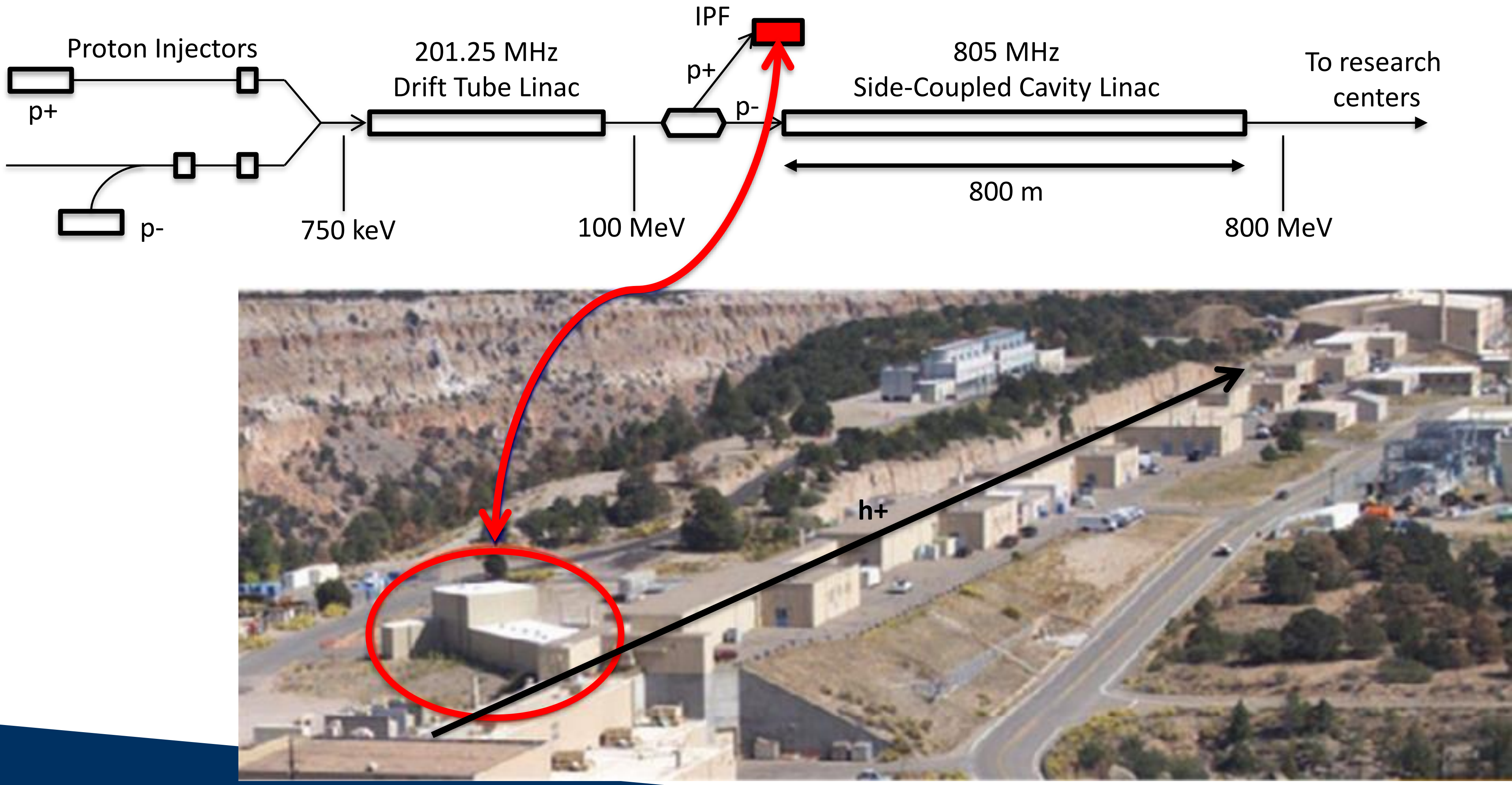

Measurements @ LANL – Nb(p,x)

- LBNL: 5 – 55 MeV / A, LANL: 45 – 100 MeV p+
- Complementary measurements explore reaction dynamics in different energy regimes, overlap region of 45-55 MeV builds confidence and consistency in results.

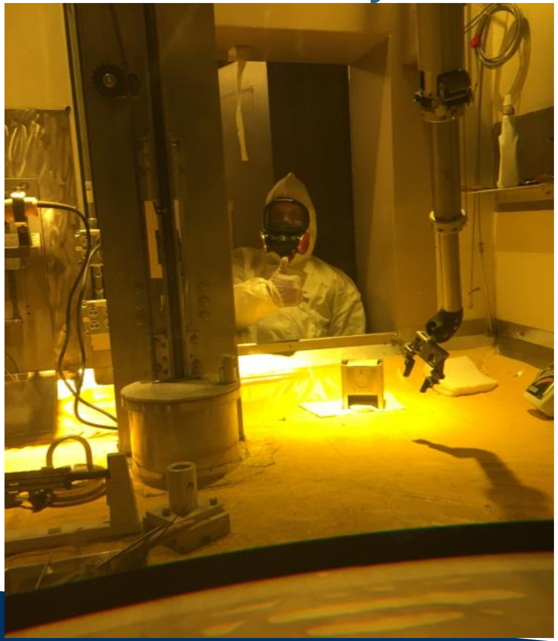

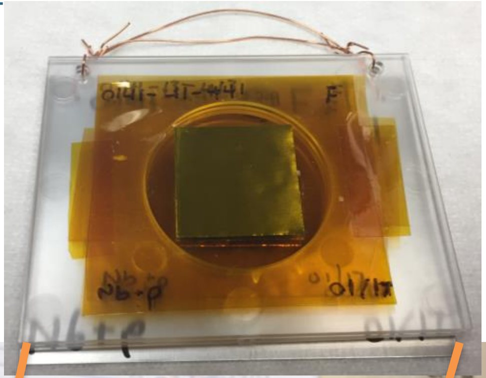

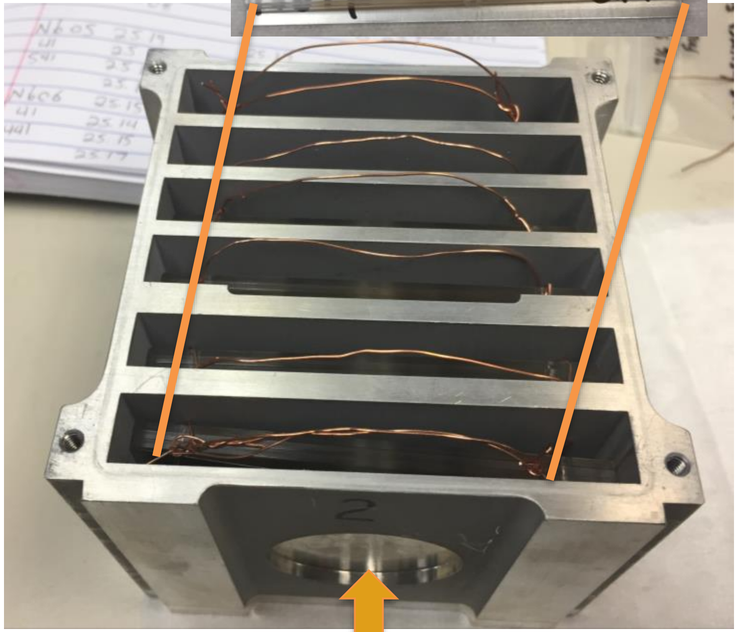

100 MeV p+

Measurements @ LANL – Nb(p,x)

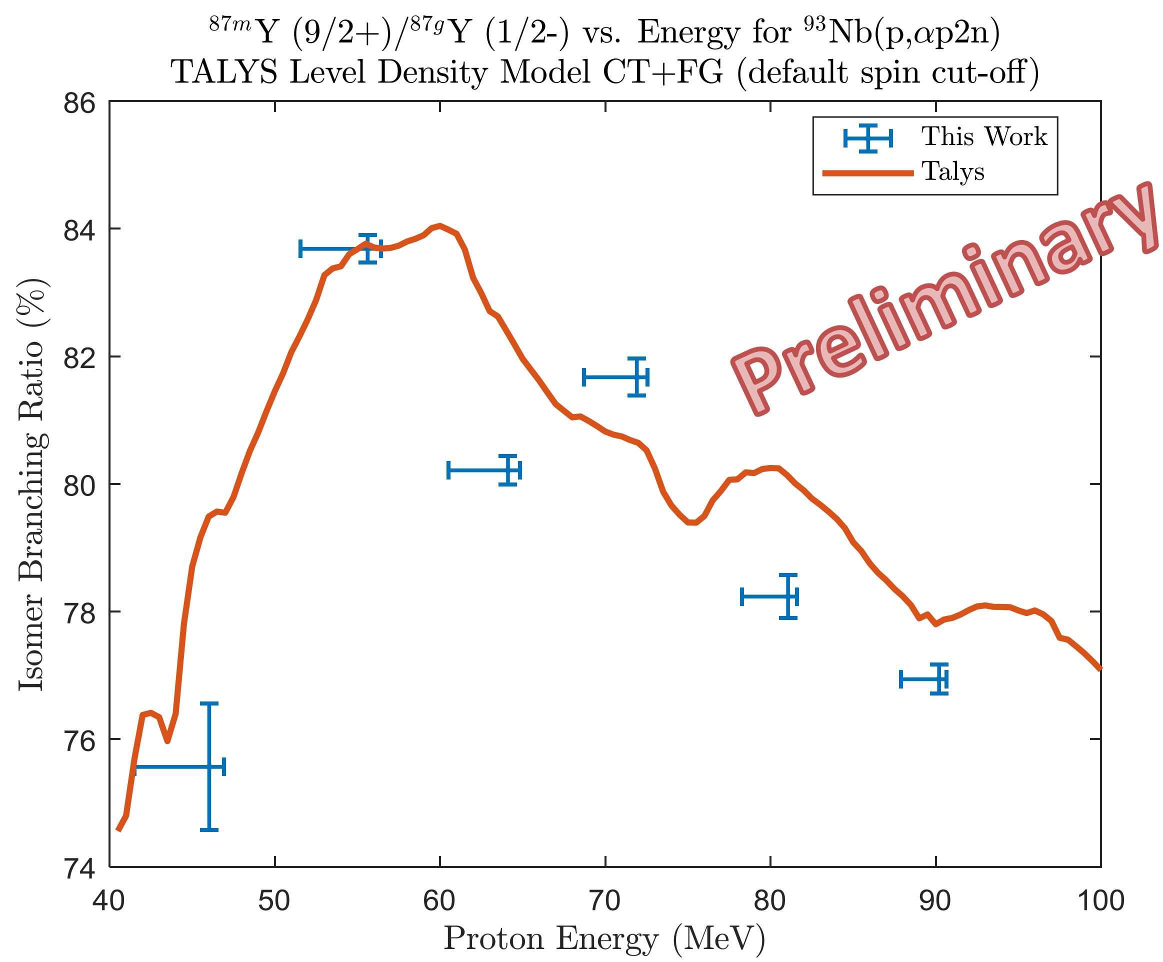

Measurements @ LANL – Nb(p,x)

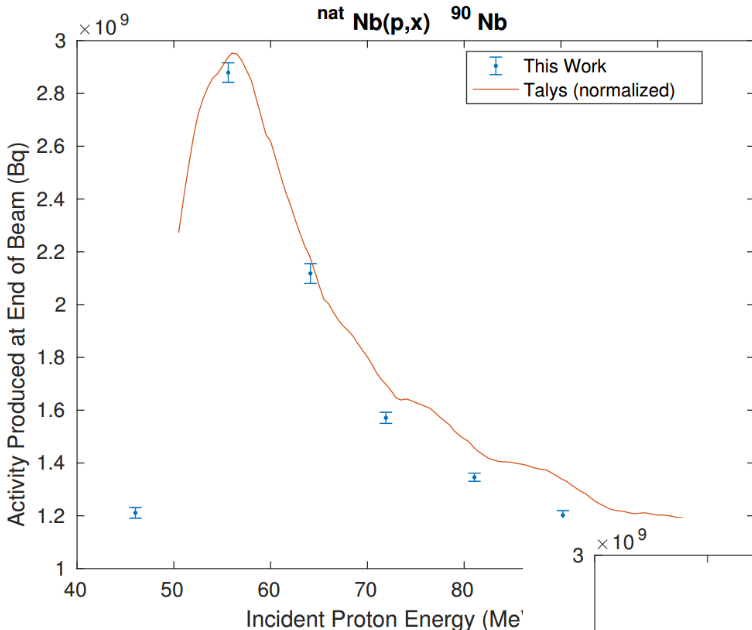

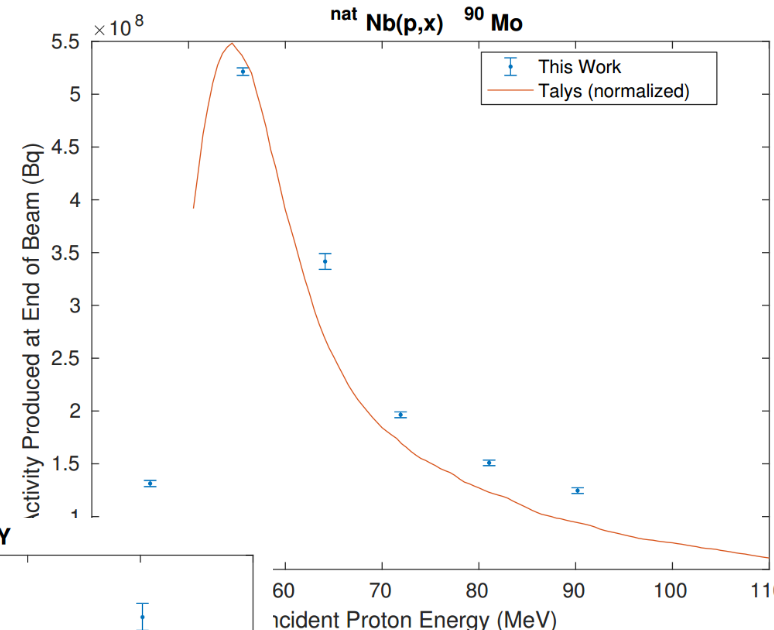

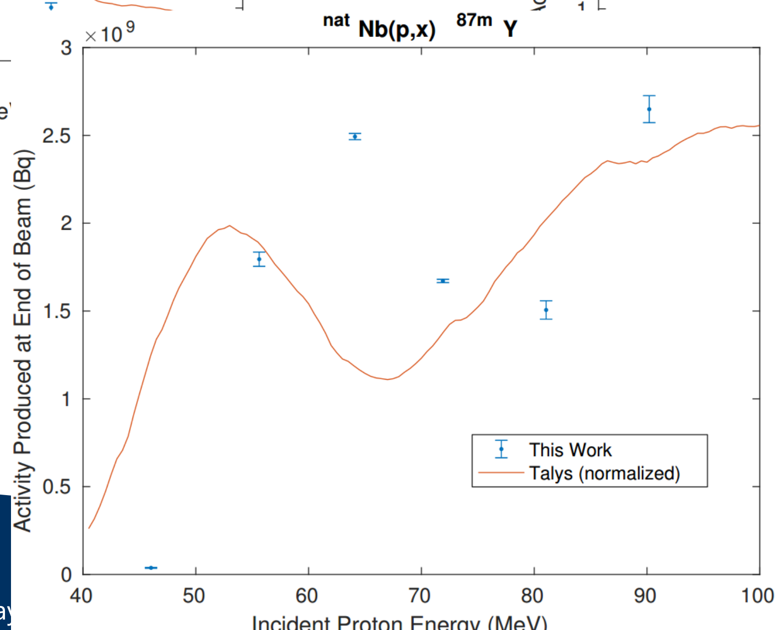

Tunable Quasi-Monoenergetic Neutron Source

LBNL

^{7}Li(p,n) Neutron Sources

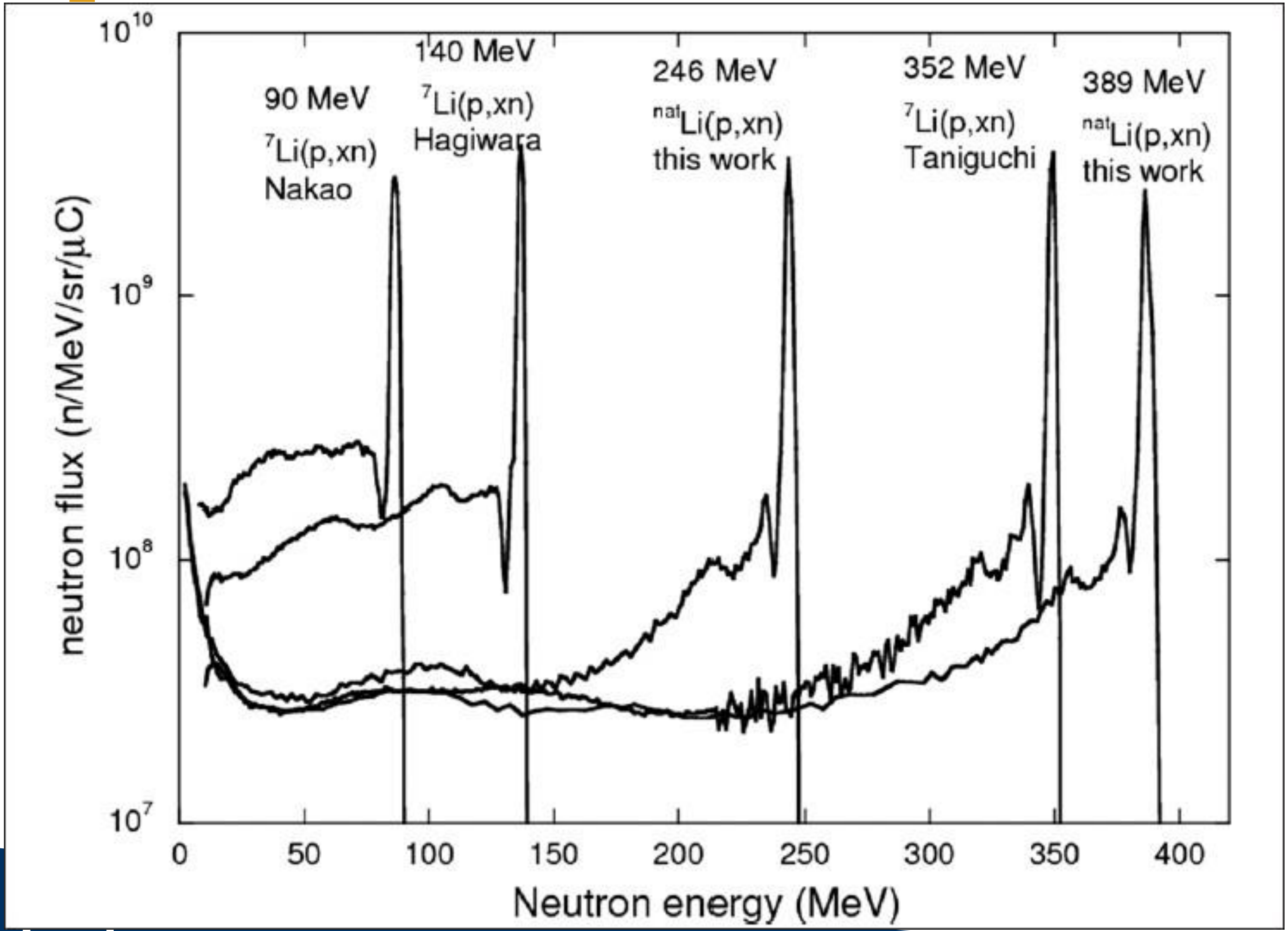

Nakamura, Takashi. *Radiation Protection and Environment* 35.3 (2012): 111.

^{7}Li(p,n) Neutron Sources

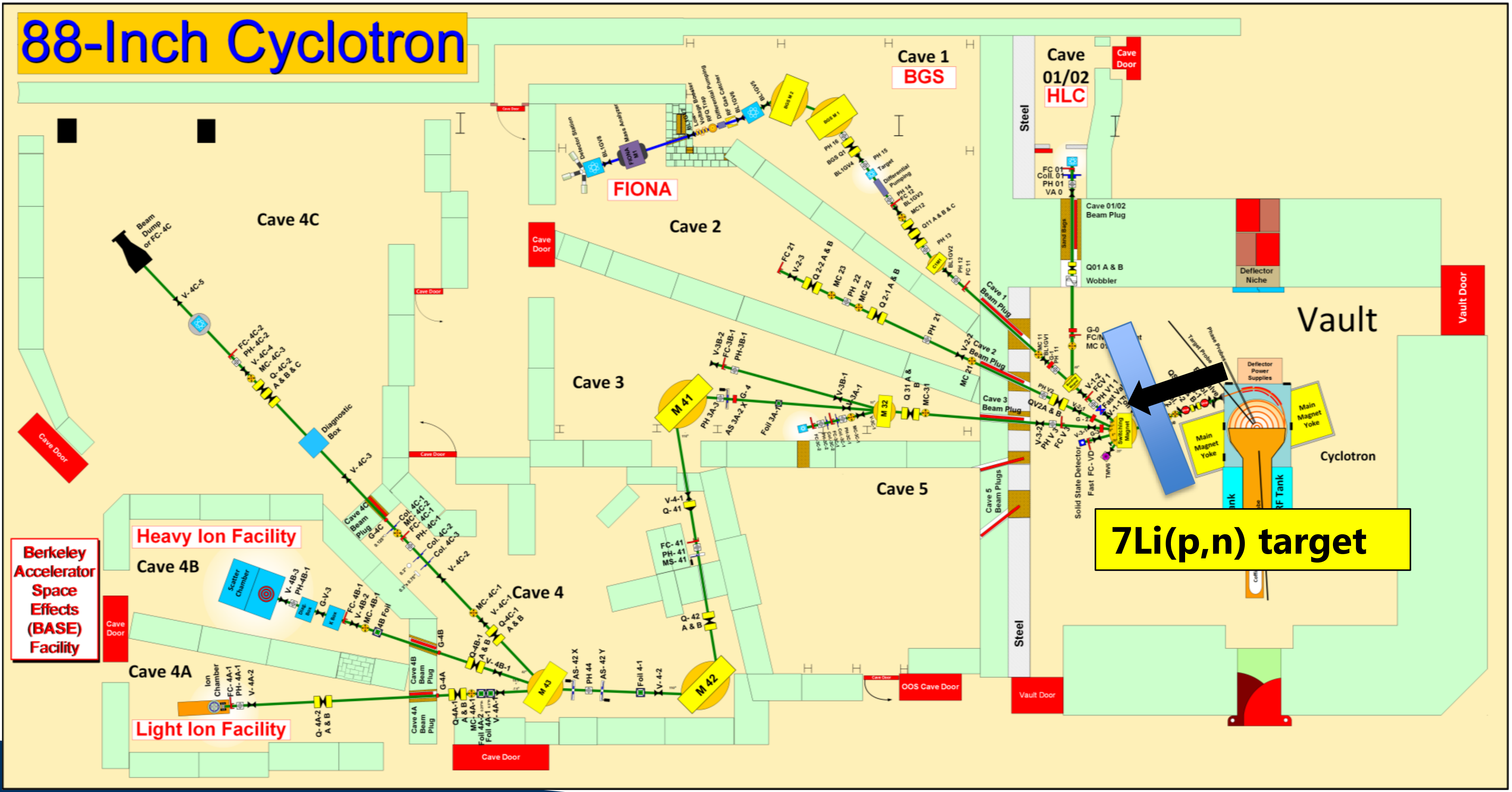

^{7}Li(p,n) Neutron Sources

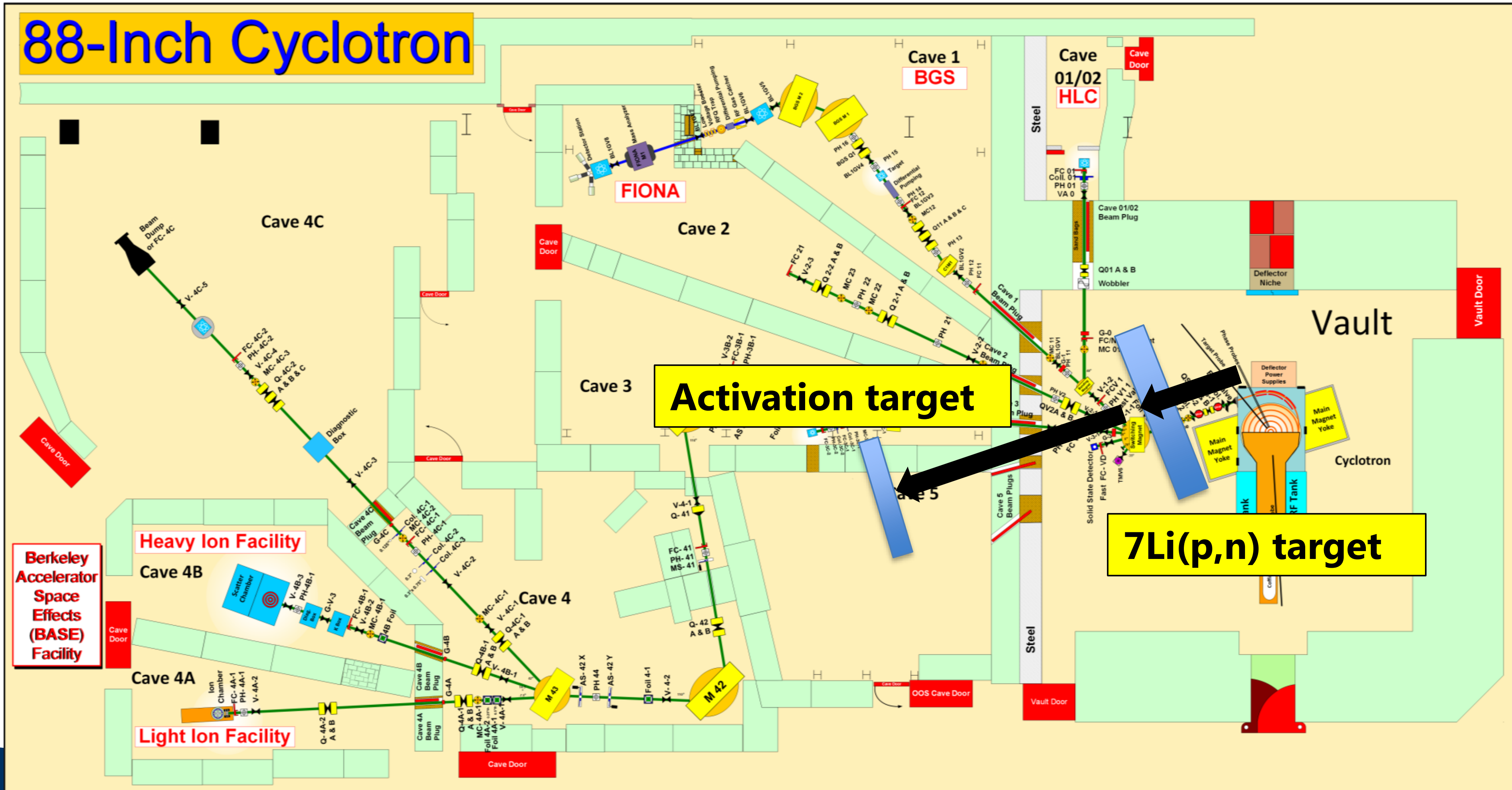

^{7}Li(p,n) Neutron Sources

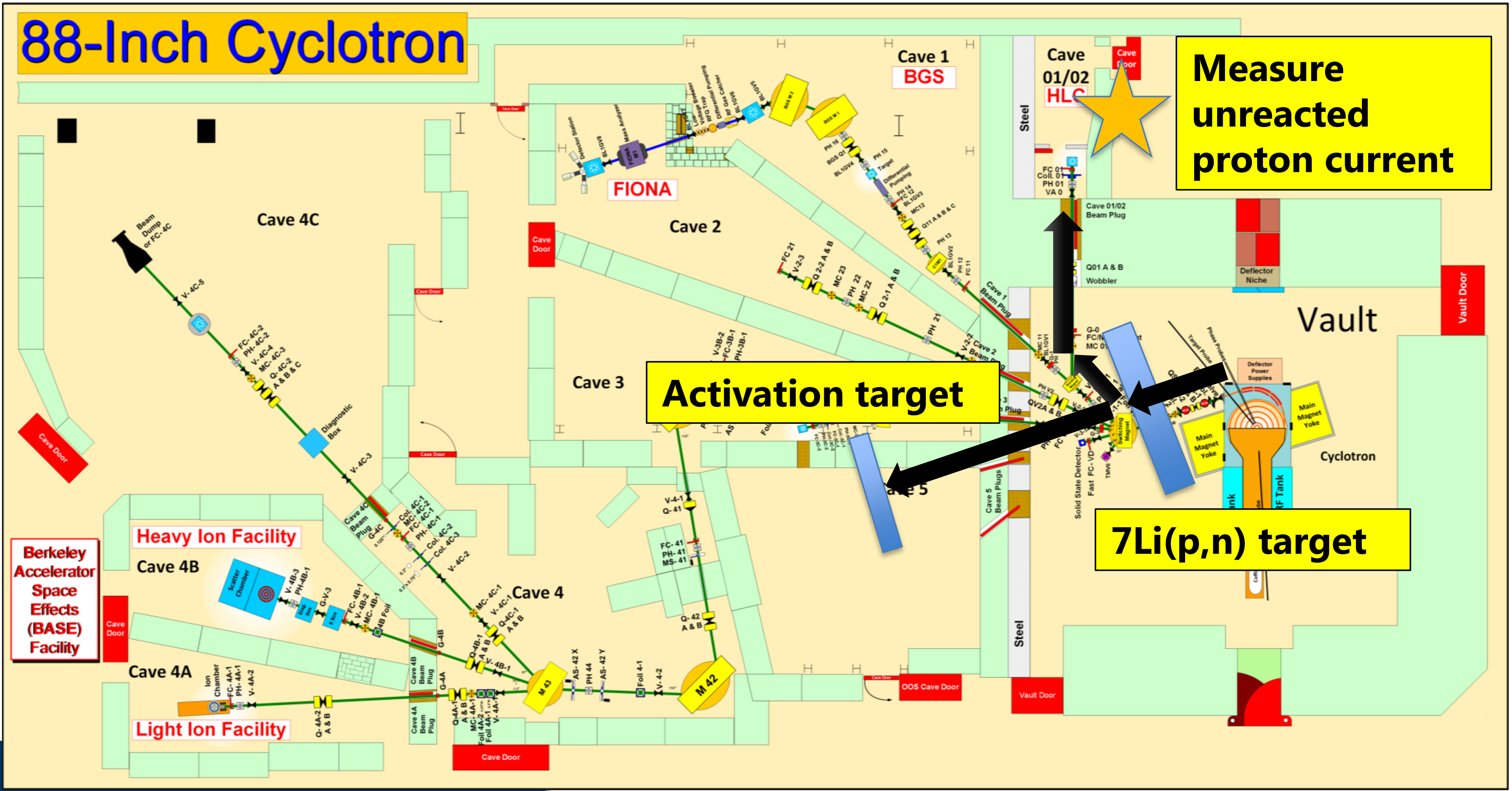

^{7}Li(p,n) Neutron Sources

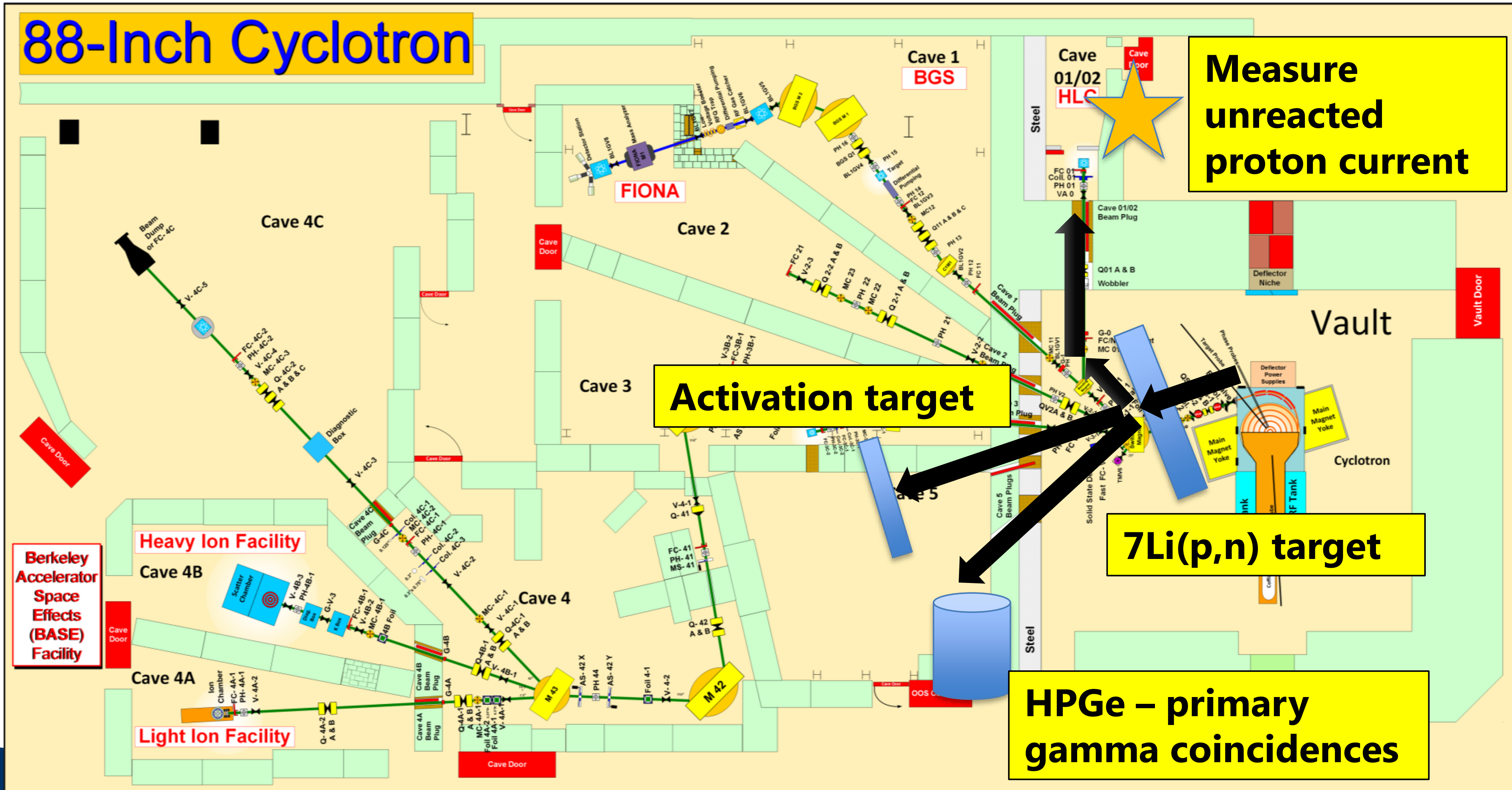

Berkeley UNIVERSITY OF CALIFORNIA

^{7}Li(p,n) Neutron Sources

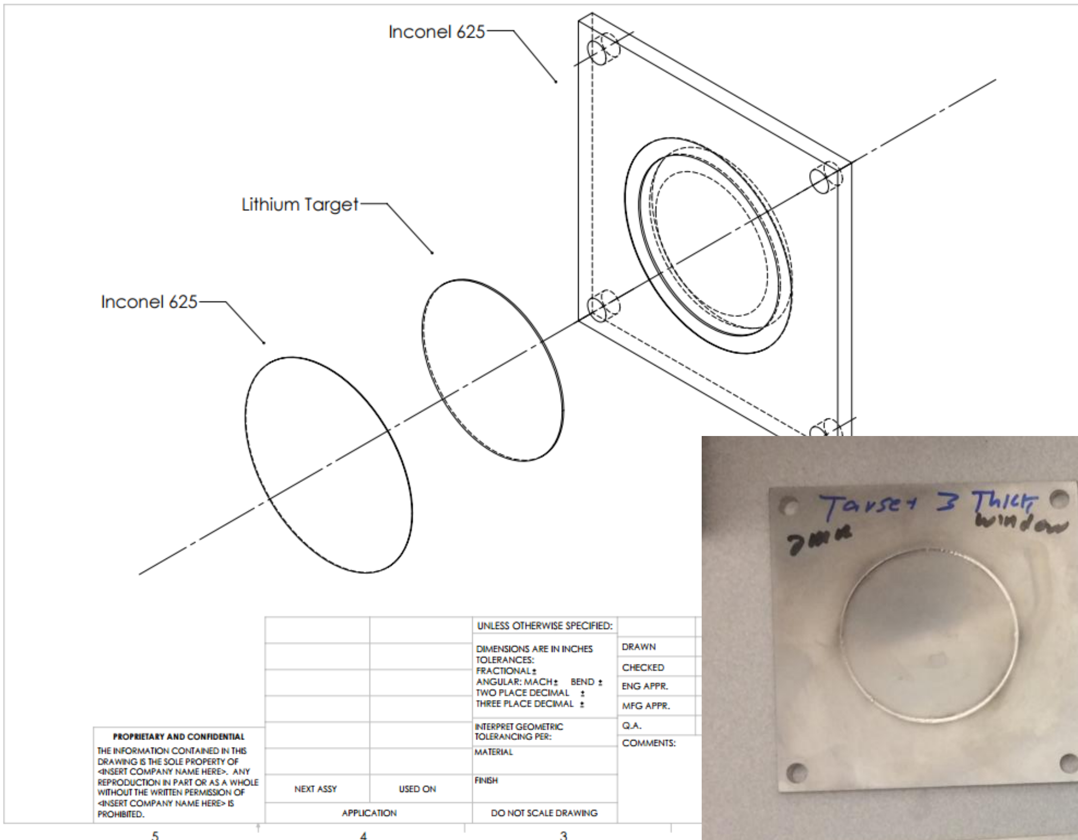

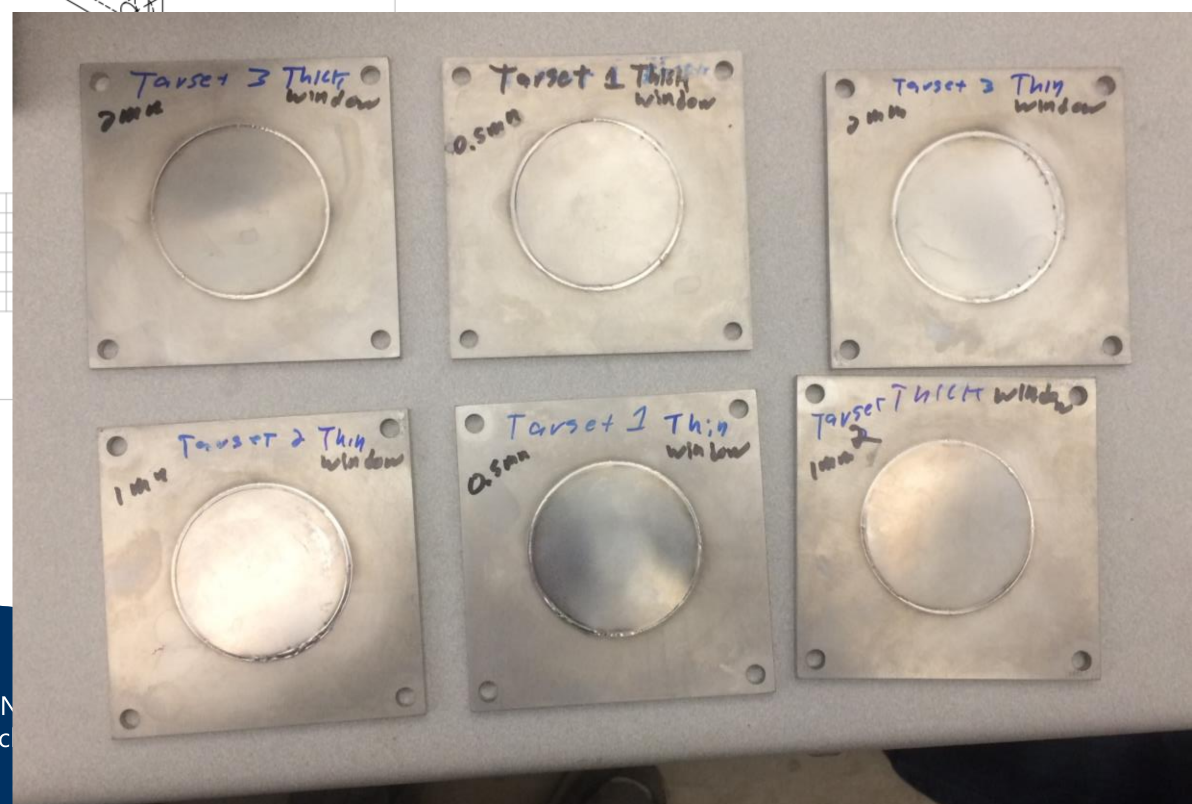

Summary

Demonstrated ability to measure $R_{spin\text{-}cut}$ in excitation function studies for emerging medical radioisotopes

- Already completed: ^{64}Cu and ^{47}Sc (n,p), Fe(p,x), Zr(d,x), Nb(p,x)
- Upcoming targets: $^{86}Sr(p,x)^{86}Y$, $La(p,x)^{134,135}Ce$, $^{177}Hf(n,p)^{177}Lu$
  - $^{7}Li(p,n)$ quasi-monoenergetic neutron source development

- Possible future candidates: Access targets previously fielded by β^{+}-Oslo in the A≈50,90, rare earth regions via (p,xn), (α,xn)

Berkeley
UNIVERSITY OF CALIFORNIA